Table of contents

AKNOWLEDGEMENTS

The work presented here was carried out in the laboratory of Professor Ola Myklebost at the Tumor Biology Department of the Institute for Cancer Research, the Norwegian Radium Hospital, Oslo University Hospital, from April 2011 to May 2012.

I wish to express my sincere gratitude to everyone who has contributed to this thesis work.

First of all, I would like to thank the Group leader Professor Ola Myklebost for giving me the chance to put myself to the test and to carry out this Master project in his wonderful research group. Thanks for giving me the advice during the writing process and for always being available.

My special thanks goes to my laboratory supervisor Dr. Else Munthe for believing in me, for always supporting my ideas, for making me feel needed, for sharing your knowledge and experience, answering all my questions, for always taking time to discuss results and experiments with a positive and enthusiastic attitude, patience and encouragement through this project. Thank you for being the best supervisor ever!

I am grateful to Eva, Silje and Iwona for always being nice, for answering my questions, for being available for whatever help I needed and for guidance during the writing. Sincere thanks to Jeanette, Anna and Russell for their precious help especially at the early stages of my Master project, and whenever a problem occurred. I am grateful to Tale for giving me technical support during the final phase of writing of the thesis.

I would like to thank Nomdo Westerdaal from SFI Flowcytometri Core Facility for helping me with sorting of the cells.

I also want to sincerely thank Mirna Therapeutics for providing let-7 miRNA mimics that made it possible to carry out this project.

Thanks to all the members of the Group for always being kind and generous in giving me support.

Oslo, May 2012

Anastassia Serguienko

ABBREVIATIONS

2-HG	2-hydroxyglutarate
ABC	Active beta-catenin
Ago	Argonaute protein
ATP	Adenosine triphosphate
bFGF	basic Fibroblast growth factor
CK1	Casein kinase 1
CMV	Cytomegalovirus
CSCs	Cancer Stem Cells
ECM	Extracellular matrix
EF1	Elongation factor 1
EGF	Epidermal growth factor
EGFR	Epidermal growth factor receptor
EMT	Epithelial-Mesenchymal transition
ER	Estrogen receptor
FACS	Fluorescence activated cell sorting
FBS	Fetal bovine serum
GAPDH	Glyceraldehyde 3-phosphate dehydrogenase
GFP	Green fluorescence protein
GSK3B	Glycogen synthase kinase-3b
HER2	Human epidermal growth factor receptor 2
HMGA2	High mobility group A2
HMLEs	Immortalized human mammary epithelial cells
IDH	Isocitrate dehydrogenase
JMJD	Jumonji C domain
MET	Mesenchymal-Epithelial transition
miRNA	Micro RNA
MMPs	Matrix metalloproteinases
mRNA	Messenger RNA
NFkB	Nuclear Factor kappa B
ON	Over night
PBS	Phosphate-buffered saline
PHGDH	Phosphoglicerate dehydrogenase
PR	Progesterone receptor
Pre-miRNA	Precursor miRNA
Pri-miRNA	Primary transcripts miRNA
PS	Penicillin streptomycin
PSAT1	Phosphoserine aminotransferase
p-Ser	Phosphoserine
PSPH	Phosphoserine phosphatase
PVDF	Polyvinylidene fluoride
RISC	RNA-induced silencing complex
RLS	RISC loading complex
RNA	Ribonucleic acid
RT	Room temperature
SDS	Sodium dodecyl sulfate
TBS	Tris buffered saline
TCA	Tricarboxylic acid cycle
TGFβ	Transforming growth factor beta
UTR	Untranslated region
α-KG	α-ketoglutarate

1. INTRODUCTION

The discovery of cancer stem cells (CSCs) was a key moment in the fight against cancer since it opened a new field of investigation and shed light on the mechanisms underlying tumor development. The CSCs may represent the true inexhaustible source of tumor cells being responsible for growth and sustenance of cancers. The challenge is to create methods to detect, classify, isolate and analyse the CSCs in order to identify new therapeutic targets that can stop their self-renewal ability.

My Master project is a part of this innovative research that is carried out in Ola Myklebost's group at the Tumor Biology Department in the Institute for Cancer Research, the Norwegian Radium Hospital, Oslo University Hospital.

1.1. Cancer stem cell hypothesis

Malignant tumors are characterized by a wide heterogeneity [1-3]. Within the tumor mass it is possible to find both tumorigenic and non-tumorigenic cells that likely provide a favourable environment for development of cancer.

In recent years it has become increasingly evident the existence of a particular type of tumor cells that are able to escape cancer therapy. These tumor cells are hypothesized to cause relapse several years after initial complete remission and could also be responsible for the high mortality of certain cancers due to their invasiveness and their capacity to rapidly metastasize. In many cases the properties of these special cancer cells resemble those of stem cells: for instance, they are able to self-sustain their growth, move across tissues and survive in hypoxic conditions. Due to these similarities with the stem cells, they were named cancer stem cells (CSC).

In normal tissues the adult stem cells sustain tissue renewal through asymmetric division. When a stem cell divides, one of two daughter cells is committed to differentiate, undergoes clonal expansion followed by terminal differentiation and becomes a tissue-specialized cell, while the another daughter cell retains stem properties and gives rise to a new asymmetric division (Figure 1):

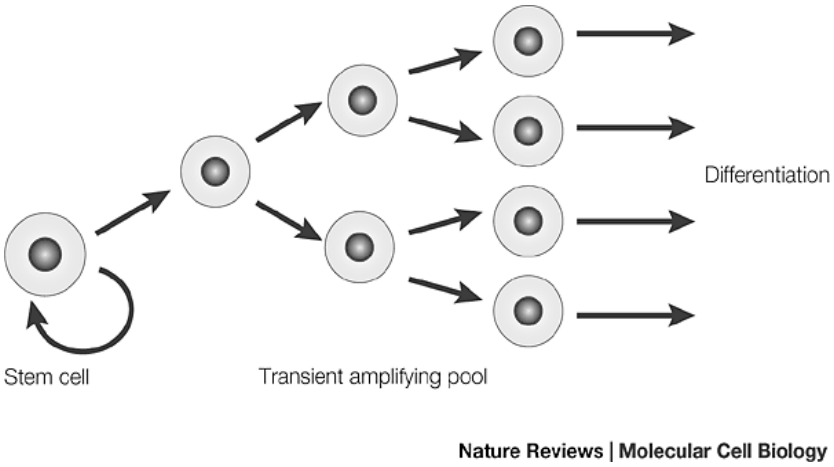

Figure 1. Stem cell asymmetric division mechanism. An adult stem cell generates two daughter cells, of which one gives rise to lineage-restricted progenitor cells that undergo clonal expansion and then terminally differentiate; while the second daughter cell replaces the mother stem cell. [Knoblich, 2001]

Stem cells capacity of long-term self-renewal, as well as the capacity to give rise to mature differentiated cell types with characteristic morphologies and specialized functions, is ensured by the expression of specific genes that are silenced in differentiated cells. In other words, one specific gene expression program confers a stem-cell phenotype and another, different gene expression program confers a differentiated-cell phenotype. Each gene expression program is obtained through epigenetic mechanisms. Just as a conductor decides the dynamic execution of a symphony, epigenetic factors govern the orchestration of DNA within each living cell. The current opinion in the scientific community (although there is no total consensus in this respect) is that the tumor mass, normally derived from a specialized tissue, can contain some cancer cells with stem-like properties. For example, the analysis of breast cancer cells grown in immunocompromized mice, has shown that only a small number of cancer cells (as few as 100 cells) had the ability to seed new tumors [2]. These cells subsequently have been identified as $CD44^{+}CD24^{-/low}$. CSCs manifest their aggressiveness not only by promoting metastatic dissemination or chemoresistance, but also by altering normal cells in the surrounding environment. It was found that embryonal carcinoma cells induce neighbouring normal prostate tissue stromal cells to acquire the characteristics of cancer-associated stromal cells, which provide a favourable environment for tumor growth [4]. Whether CSCs arise directly from transformed adult stem cells or from transformed differentiated cells, and if these modifications are spontaneous or stroma-induced, remains unclear. It is thought that the generation of CSCs in carcinomas, tumours of epithelial origin, requires a kind of epithelial-to-mesenchymal transition (EMT) [5]. A statistical study carried out on the breast cancer cells, showed that in aggressive triple-negative breast cancer (that does not express Estrogen receptor (ER), Progesterone receptor (PR) nor Human Epidermal Growth Factor Receptor 2 (HER2)) the three mesenchymal markers vimentin, Epidermal Growth Factor Receptor (EGFR) and Nuclear factor

kappa B (NF-kB) were significantly increased compared to the non triple-negative and less aggressive breast cancer types [6]. In another study it has been shown that breast cancer cells expressing the mesenchymal marker Tenascin C, which is an extracellular matrix protein, form the invasive front of the tumor and are able to efficiently metastasize to the lungs with a short relapse-free time [7].

1.2. The Epithelial-to-Mesenchymal Transition

Epithelial cells perform numerous biological functions, like to cover surfaces, protect the underlying structures and organs and play different tissue-specific roles. To fulfil these functions, the cells are provided with cell-cell junctions that ensure apical-basal polarity and allow the generation of continuous compact layers. By their basal membrane, epithelial cells are anchored to the basal lamina, a thin mat of specialized extracellular matrix (ECM), that supports epithelial cell population. By contrast, mesenchymal cells are single, independent cells characterized by anterior-posterior polarity. Mesenchymal cells are embedded in the interstitial ECM inside which they are able to move easily. The process that allows epithelial cells become mesenchymal is referred to as epithelial-to-mesenchymal transition (EMT).

The EMT is a physiological process present in multi-cellular organisms that promotes a reorganization of germ layers and tissues during embryonic development leading to the morphogenesis [8]. The primary EMT occurs during formation of the three embryonic germ layers (endoderm, mesoderm and ectoderm) from a zygote.

The most significant changes upon EMT involve the loss of tight and adherens junctions and, as a consequence, loss of apical-basal polarity. At the molecular level these changes include: a switch from E-Cadherin to N-Cadherin, substitution of epithelial integrins with mesenchymal ones, remodeling of actin cytoskeleton into stress fibers, which accumulate at areas of cell protrusions; replacement of epithelial intermediate filaments by vimentin and expression of matrix metalloproteases (MMPs) [9]. All these changes allow the cells to detach, degrade the basement membrane and to move (Figure 2).

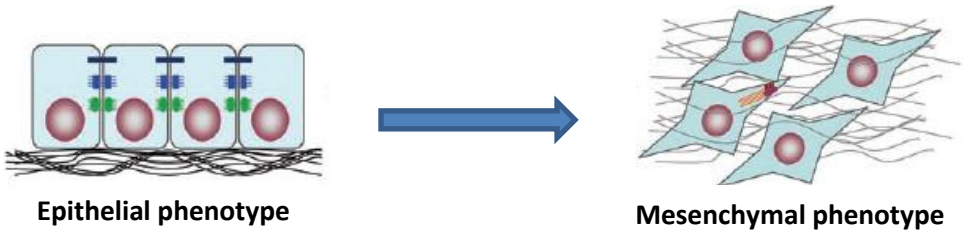

Figure 2. Schematic representation of EMT. Epithelial cells (cuboidal in this picture) undergo EMT and become migratory spindle shaped cells. Whereas epithelial cells are characterized by the apical-basal polarity and their basal membrane takes contact with a basal lamina, mesenchymal cells have an anterior-posterior polarity and are embedded into loose interstitial matrix, where they move [Jian Xu et al, 2009].

The secondary EMT occurs in late embryogenesis stage, organogenesis (ventral somite de-epithelialization to form the sclerotome, endocardial endothelial cells de-epithelialization to form the endocardial cushions etc.) [8], during embryo implantation in higher primates when the extravillous cytotrophoblast undergoes EMT, or during branching morphogenesis in the mammary gland. The EMT program can be activated also in adult tissues under particular conditions like, for instance, the epithelialization stage of wound healing or in a chronic inflammatory processes leading to the fibrosis of tissue, when the normal epithelial parenchyma is replaced by fibroblast derived from the epithelial cells trough EMT, or in tissue regeneration [10]. The secondary EMT is often partial [11]. The best examples of partial EMT are represented by collective migration during wound healing, branching morphogenesis or vascular sprouting. Here, cells use the same mechanisms for motility and invasion as a single cell does, but move in clusters or sheets [12]. The leading cells remain physically and functionally connected to surrounding cells by the adherens junctions, but, at the same time, exhibit a capability of directed cell movement, of development of cell protrusions and loss of apical-basal polarity that typically characterize EMT [12]. Mechanisms of collective migration may also be used by cancers to spread, as shown in rhabdomyosarcoma, endometrial carcinoma, colorectal or breast cancer [12-14]. Improper re-activation of pathways mediating EMT in cancer cells can give rise to metastatic cells. At a certain point, invasive tumor mass crosses the basement membrane and invades the nearby surrounding stroma. Single cells or small cell clusters can detach from the tumor and enter the blood or lymph stream [14]. So, how are distant metastasis generated? How do one or few undetectable cancer cells survive and cause the relapse several years after recovery? Features of EMT have been observed in breast [15], colon [16], lung [17], ovarian [18] and esophageal cancers [19]. Huge amount of research done in this area has shown that aggressive metastatic cell lines are characterized by poor degree of differentiation and by activation of so-called fetal oncogenes (genes able to induce tumor

formation) that play an important role in embryogenesis, but are normally silenced in adult epithelial cells, like HMGA2, Twist, Nanog and Snail. It was hypothesized that epithelial cells in the primary tumor undergo EMT and thereby contribute to tumor progression and metastasis. However, EMT usually does not occur homogenously across the whole tumor. In colon cancer, for example, it was shown that cells exhibiting mesenchymal properties specifically localized to the periphery of the tumor [16], likely due to exposure to signals from the tumor microenvironment [20]. Also the microenvironment can induce EMT in surrounding epithelial cells. For example, senescent fibroblasts can acquire a pro-inflammatory phenotype and become able to promote tumor progression, in part by inducing an EMT in nearby pre-neoplastic epithelial cells [21].

The reverse process, mesenchymal-to-epithelial transition (MET), also occurs during embryogenesis and allows the secondary epithelium to form. The EMT fits into a broader concept of epithelial plasticity and is divided in 3 main types [22] (Figure 3).

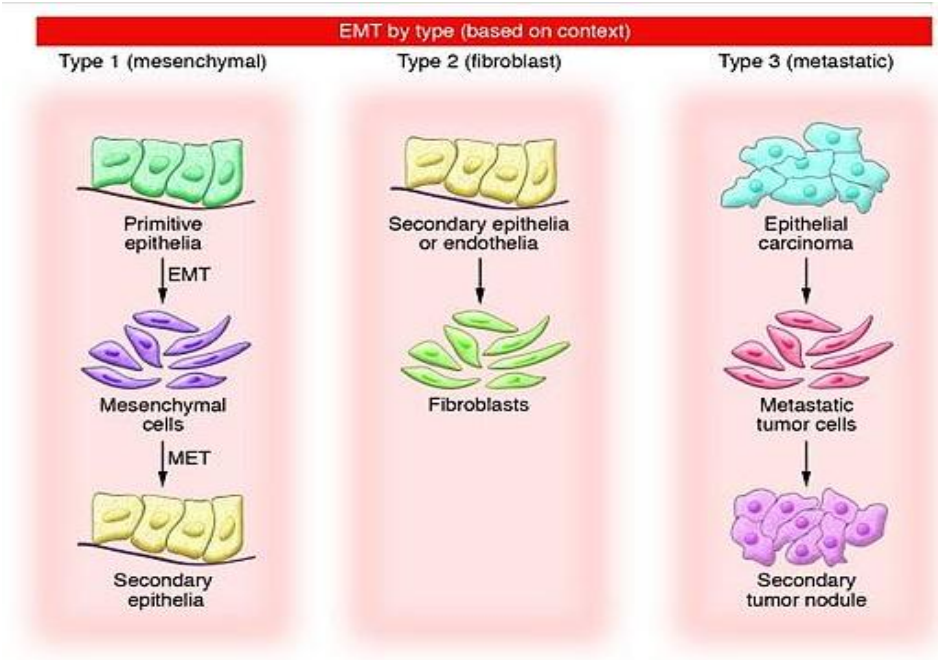

Figure 3. Types of EMT. Type 1 EMT: required for dispersing cells in embryo, occurs during implantation, embryo genesis and organogenesis. Mesenchymal cells generated by this type of EMT are able to undergo the reverse process, MET, to form secondary epithelia that will give rise to different specialized epithelial tissues.
Type 2 EMT: associated with wound healing, tissue regeneration and organ fibrosis. In this EMT epithelial cells are induced to convert into fibroblasts. Persistent inflammation can lead to organ destruction where tissue-specific epithelium is substituted by fibrous tissue formed by fibroblasts. **Type 3 EMT:** involved in metastasis formation. It is thought to be a process by which the transformed epithelial cells of primary tumor acquire the mesenchymal features like motility, contractility, ability to disrupt the basal lamina, loss of basolateral adhesion etc, that allow them to colonize new distant sites.
(adapted from Zeisberg et al., 2009)

Similar process exists also in cancer, it was observed that secondary tumors derived from migratory cancer cells can have a histopathological profile similar to the primary tumor from which they arose [23, 24]. This suggests that cancer cells that have undergone EMT are also able to undergo MET. Metastatic cancer cells that have undergone EMT and colonized distant site, can either acquire epithelial characteristics of the surrounding tissue, different from primary tumor (Figure 4) or retain the mesenchymal phenotype, depending on the microenvironment of metastatic site [25].

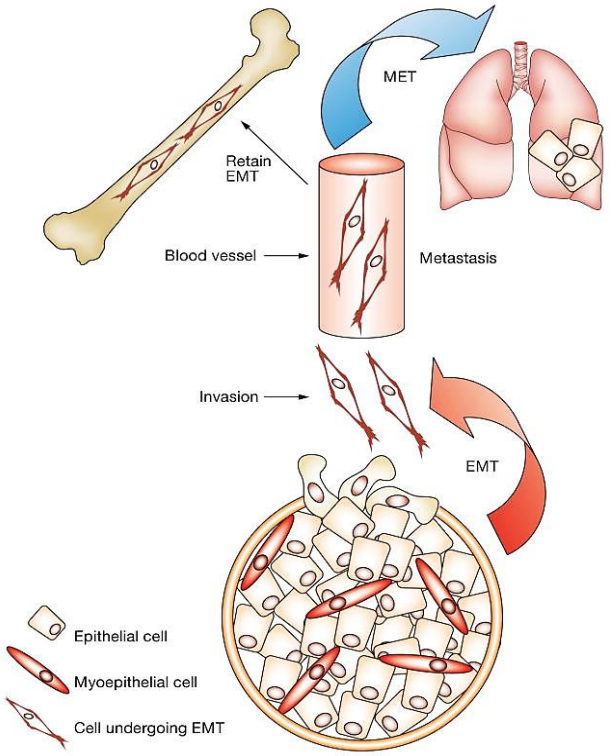

Figure 4. Migration of metastatic cells to different anatomic sites. The cells with the acquired mesenchymal feature that end up in the bone, retain their mesenchymal phenotype, however the cells that stop and form a colony in the lung, upon influence of surrounding epithelial cells, undergo MET. This picture reflects the powerful effect exerted by the microenvironment on the tumor. [Turley et al. 2008].

1.3. Genetic regulation and biochemical mechanisms of EMT in cancer.

Acquisition of a mesenchymal phenotype involves global changes in expression of genes and proteins. Many genes that are crucial for embryogenesis or adult stem cell maintenance become deleterious if expressed in adult differentiated cells. These genes play an essential role in the formation and development of a new organism or in tissue regeneration. By conferring mesenchymal properties to epithelial cells (that otherwise do not cross basement membranes), these genes enable them to move to a distant site, to position themselves correctly and to give rise to a new organ or structure. Through the same mechanism these genes allow epithelial cells to move to the site of injury and cover the wound. What all these genes do, is to induce the EMT in epithelial cells. Among the most well studied inducers of EMT are the signaling molecules Cripto, TGF-β and

Wnt as well as transcription factors such as Snail, Slug and Twist. In many aggressive epithelial tumors they are re-expressed. For example, Cripto is overexpressed in 80% of infiltrating breast carcinomas [26], while Twist is overexpressed and associated with nodal invasion in colorectal cancer [27] and with distant metastasis in esophageal squamous cell carcinoma [28]. Interestingly, some of the most important EMT-associated genes like *Twist*, *Snail*, *HMGA2*, *FSP1*, *β-Catenin*, *Vimentin*, *α-SMA*, *Ets-1* and *ZO-1* contain in their promoter a *cis*-regulatory element called fibroblast transcription site-1 (FTS-1), suggesting their simultaneous activation within the same genetic program [22]. However, the transcription factors Twist and Snail can induce EMT independently. Experiments performed on immortalized non tumorigenic human mammary epithelial cell line (HMLE) showed that ectopic expression of Twist or Snail generates cells with a fibroblast-like morphology. Furthermore, these cells have down-regulated epithelial markers such as E-cadherin, and up-regulated mesenchymal markers such as N-cadherin, vimentin and fibronectin. They also have the capability to form mammospheres in soft agar and tumors *in vivo* [5]. Cells with similar properties were isolated from different neoplastic tissues and referred to as cancer stem cells [29].

Another important EMT inducer, TGF-β1, initiates and maintains EMT in a variety of physiological, as well as pathological, contexts [30]. In addition, TGF-β1 mediates transient EMT associated with wound healing, which is promoted by inflammatory processes. Such EMT reverts once the inflammation is stopped and the stimulus is removed. Different pathways, such as Ras/MAPK, PI3K/Akt and TGFβ, all share a common end point: repression of E-cadherin [9, 31].

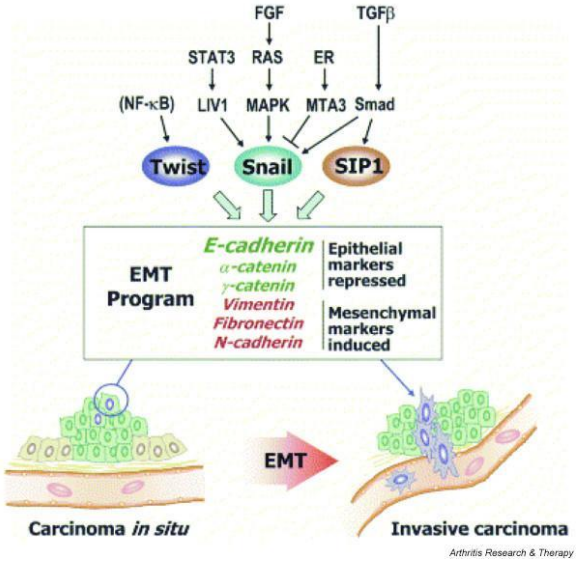

Figure 5. Some of the main pathways involved in EMT. At an early stage tumor cells still maintain epithelial features similar to the normal epithelium. Re-expression of master regulators of EMT, such as the transcription factors Twist, Snail, and SIP1, leads to changes in gene expression profiles and cellular phenotype. New properties conferred by expression of mesenchymal markers like vimentin, fibronectin, N-cadherin and by repression of epithelial ones, permit cells to cross the basal membrane and vascular endothelium and reach distant sites through blood stream [Zvaifler, 2006].

One of the most important pathways that promotes EMT and is associated with CSC generation is the Wnt signaling pathway. There are two types of Wnt signaling pathway: canonical and non canonical. The canonical Wnt pathway functions through β-catenin, while two non-canonical pathways are β-catenin independent [32]. In this thesis I will focus only on the canonical one. Normally, Wnt pathway is only active during embryogenesis where its major role is body axis specification and morphogenesis. When re-activated in adult differentiated cells, it leads to malignant transformation. The presence of active Wnt signaling in cancer confers elevated aggressiveness, typical of cells that have acquired a mesenchymal phenotype [33, 34]. The whole pathway consists of a large protein network that range from extracellular signaling molecules to transcription factors. Once the Wnt ligand has bound to the Frizzled receptor on the cell surface, the signal is transmitted inside the cell and triggers a cascade of events which, in turn, leads to the activation of Wnt target genes (Figure 6).

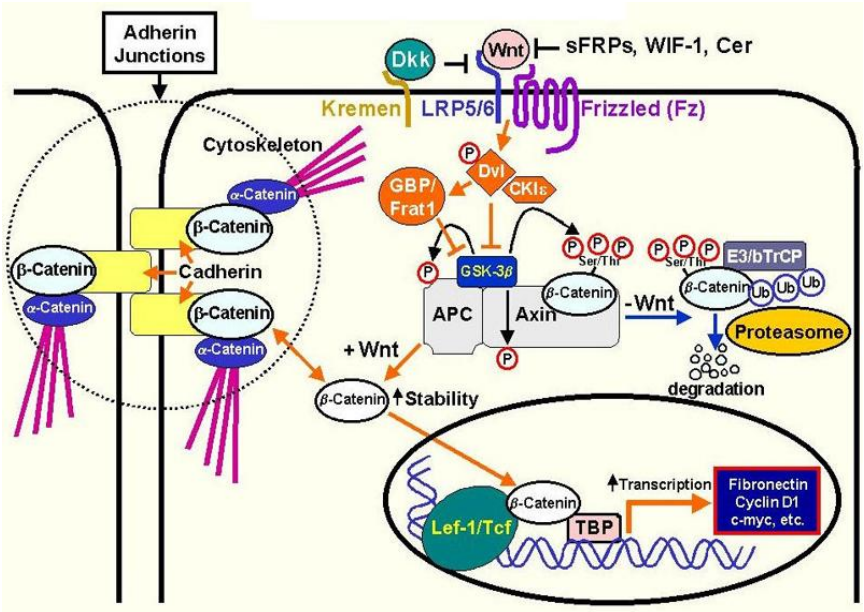

Figure 6. Schematic overall representation of the canonical Wnt pathway. In the absence of Wnt signaling molecules cytoplasmic β-catenin is sequestered by degradation complex, phosphorylated and degraded by the proteasome. Upon binding of Wnt molecules to the LRP5/6 and the Frizzled receptors, β-catenin is released from the degradation complex, stabilized and traslocates into the nucleus where it binds to the promoters and acts as a transcription factor activating genes involved in cell growth and cell cycle progression. [Howard et al. 2003].

The key protein of intracellular signaling of Wnt pathway is β-catenin. In epithelial cells β-catenin is an integral part of adherens junctions, which provide a strong mechanical attachment between the cells. Within the junctions, β-catenin functions as a bridge by binding to E-cadherin on the one side and to the actin fibers, via α-catenin, on the other (Figure 6). There is also a small "free" cytosolic fraction of β-catenin, which in the absence of active Wnt signaling is kept at a low level through proteasomal degradation. The marker for this proteasomal degradation is given by the

phosphorylation of N-terminal Serine 33/37 and Threonine 41 residues on β–catenin, mediated by glycogen synthase kinase-3b (GSK3B) [35]. Phosphorylation of these residues requires prior phosphorylation of Ser-45 by casein kinase I [36]. When the canonical Wnt pathway becomes activated, β–catenin is dephosphorylated on Ser33, Ser37 and Thr41 residues and thereby no longer degraded. Stabilized β-catenin accumulates in the cytoplasm and migrates to the nucleus where it acts as a activator of transcription. Among the known Wnt target genes are *CCND1* (encoding Cyclin D1), *CMYC*, *FN1* (encoding fibronectin) and some MMPs.

1.4. Cancer cell metabolism

Cancer affects all aspects of the cell's life. Among them, cell metabolism plays one of the most important roles. All living organisms need energy to survive, and this energy for all of those which are not plants, algae or cyanobacteria, is derived from nutrients like, for example, glucose. The energy extracted from glucose is stored in the form of adenosine triphosphate (ATP) molecules. In aerobic organisms the last step of glucose metabolism, oxidative phosphorylation, leading to the ATP production, takes place in the inner mitochondrial membrane and requires oxygen. An alternative pathway to produce ATP, fermentation, occurs in the cytoplasm and does not require oxygen. In animal cells, under hypoxic conditions, glucose can be converted into lactate through the lactic acid fermentation process. When lactic acid fermentation occurs in anaerobic conditions it is called anaerobic glycolysis (Figure 7) [37]. In proliferative tissues, i.e. embryonic, in some differentiated tissues/cells, e.g. brain, retina or erythrocytes or in cancer cells glucose metabolism occurs in the cytosol through lactate pathway even in the presence of oxygen. For this reason the lactic acid fermentation in aerobic conditions was called aerobic glycolysis. The ATP yield of aerobic glycolysis is 18-fold lower than those of oxidative phosphorylation (2 ATP molecules against ~36 ATP for one molecule of glucose), but glycolytic rates of aerobic glycolysis are up to 200 times higher than those of oxidative phosphorylation. This allows rapidly growing cells to meet the demands for ATP. Cancer cells share with fetal tissues the ability to proliferate and to build up the biomass very fast. In addition, they are also able to survive in the hypoxic microenvironment often present inside tumor bulk or during metastatic dissemination of tumour cells. This capacity is ensured by a phenomenon called the Warburg effect: the switch from oxidative phosphorylation to lactic acid fermentation in the presence of oxygen. This phenomenon is named after the Nobel laureate Otto Heinrich Warburg, the scientist who, in 1924, postulated a hypothesis that cancer cells predominantly produce energy by aerobic glycolysis. But the effect of oxygen on the fermentation

process was discovered much earlier, in 1857, by Luis Pasteur. He observed that facultative anaerobes yeast grown in the presence of oxygen, had an increased cell growth, while the fermentation rate slowed down. This observation was referred to as the "Pasteur effect".

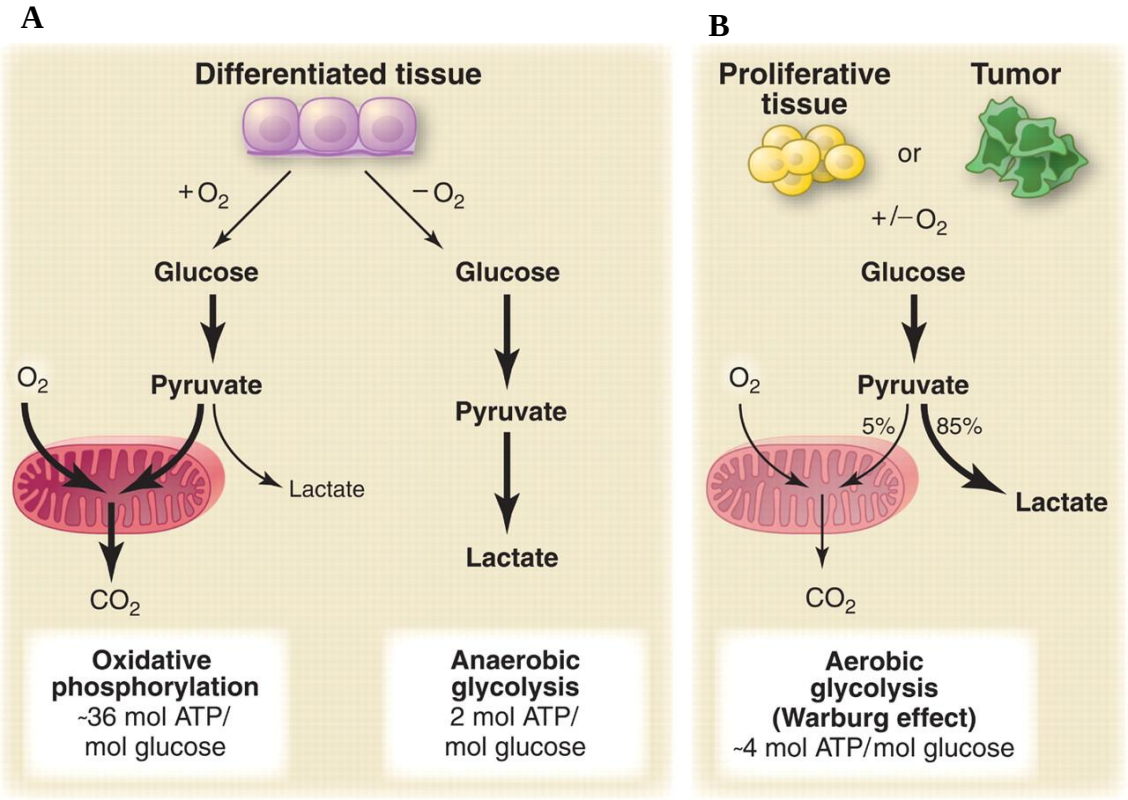

Figure 7. Two main pathways of glucose metabolism. In the majority of differentiated tissues, in the presence of oxygen, the ATP production occurs only in mitochondria through the mechanism of oxidative phosphorylation that yields ~36 molecules of ATP for each molecule of glucose (**A**). When the flux of oxygen is not sufficient, like for example during strenuous exercise, the metabolism switches to anaerobic glycolysis, that occurs in the cytosol and produces lactate as final product. In contrast, in rapidly proliferating tissues or in cancers, even in the presence of oxygen the cells use preferentially lactate pathway to generate ATP (Warburg effect) (**B**) [Heiden et al. 2009].

The lactic acid produced during aerobic glycolysis is excreted out by the cell and undergoes different fates in different tissues. For instance, lactate produced in muscle cells is transported to the liver where it is converted back to glucose. However, the biological role of aerobic glycolysis in rapidly proliferating cells is rather controversial. The analysis of data from different published studies for a total of 31 cancer cell lines showed that the average of ATP contribution from glycolysis is only 17% [38]. Moreover, there are evidences that suggest that a main function of the glycolytic pathway in proliferating cells is to supply glycolytic intermediates for biomass generation [37].

1.5. MICRO RNAs: The basics

MicroRNAs (miRNA) are small non coding RNAs of 18-24 nucleotides (nt), evolutionarily conserved across phyla from nematodes to humans, that play regulatory roles in the cell. *In silico* analysis estimated that in human cells there are ~ 1000 different microRNAs that regulate the expression of 30-70% of all the protein-coding genes [39, 40]. miRNAs are divided into 48 families based on their **seed sequence**: the first 2-8 nucleotides (nt) at their 5' end. miRNAs perform their regulatory function by pairing their seed sequence to the 3` untranslated region (UTR) of target RNA messengers (mRNAs) (Figure 8). Although perfect match to the seed sequence is necessary, the total complementarity of whole miRNA is not required. The imperfect nature of mRNA:miRNA alignment enable a single miRNA to target ten to hundreds of mRNAs. They are able to inhibit mRNA translation either by inducing degradation of target mRNA or by interfering with the translational machinery, thus down-regulating the protein level of the target genes.

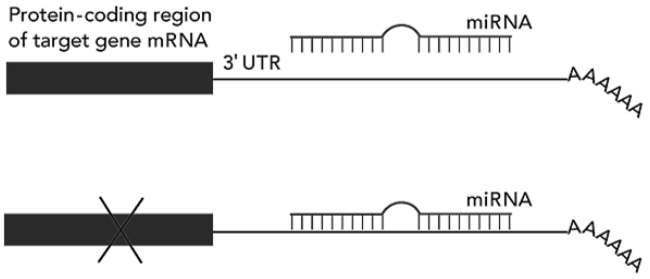

Figure 8. Pairing of miRNA to mRNA. Mature miRNA pairs to the 3'UTR of target mRNA and inhibits translation. The loop in the middle shows the imperfect nature of binding. (from Victor Ambros www.laskerfoundation.org)

The majority of miRNAs are transcribed by RNA Polymerase II. Near 50% of miRNA transcripts derive from non-protein coding genes, while an additional 40% are located within introns of protein coding genes. The primary transcripts (pri-miRNAs), which can be up to several thousands of nucleotides long, are capped at the 5' end and polyadenylated at the 3'end. The maturation of miRNAs consists of two subsequent processings. Pri-miRNAs contain a distinctive stem loop structure and are processed by Drosha/DGCR8 microprocessor complex to 60- to 100-nt hairpin fragments with a characteristic 2-nt overhang at the 3' end, referred to as precursor miRNAs (pre-miRNAs) (Figure 9) [41].

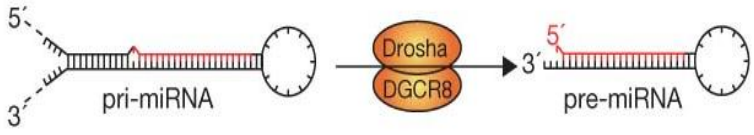

Figure 9. Pri-miRNA processing. The microprocessor complex Drosha/DGCR8 cleaves the pri-miRNA, releasing the shorter stem-loop pre-miRNA with 2-nt overhang at the 3' end.

Pre-miRNAs are transported from the nucleus to the cytoplasm by Exportin 5 where they are further processed by the Rnase III Dicer to generate approximately 22-nt unstable double-stranded mature miRNA (Figure 10) with a 2-nt overhang at the 3' ends.

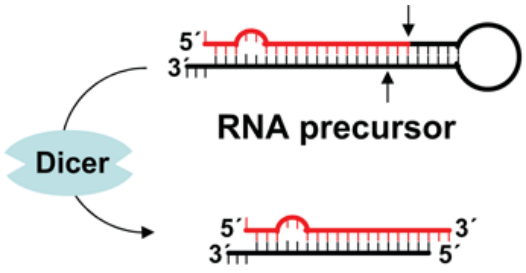

Figure 10. Pre-miRNA processing. Dicer cleavage generates a mature miRNA: short double-stranded fragment of 18-24 nt (from Dianne Schwarz. http://www.sciencemag.org/site/feature/data/prizes/ge/2006/schwarz.xhtml).

The mature miRNA is loaded to the RNA-induced silencing complex (RISC) where the passenger strand is degraded and guide strand is used to target mRNA and to inhibit translation. The mechanism of strand selection is not completely understood, however, the guide strand generally exhibits lower thermodynamic stability of the 5' end [42, 43].

A perfect pairing of the seed sequence with the target mRNA is required for the efficient translation inhibition. Extensive base-pairing with perfect alignment at the center of the miRNA leads to endonucleolytic cleavage [42]. An endonucleolytic cleavage is performed by the catalytic component of the RISC complex, the Argonaute protein 2 (Ago2), the only one among the four vertebrate Ago proteins that has endonuclease activity. Because of these limitations, only a few animal miRNA targets that are silenced trough endonucleolytic cleavage were reported [40]. However, miRNA-mediated Ago-independent degradation of target mRNAs also was found. Such degradation is thought to occur through deadenylation of mRNAs.

Little is known about how microRNAs are regulated at the transcriptional and post-transcriptional levels besides the maturation process. The only known specific factor that mediates post-transcriptional regulation of miRNAs is the RNA-binding protein Lin28 (Lin28A and Lin28B), that

inhibits the processing of the *let-7* family by binding to the loop-structure of pri- and pre-miRNAs [44].

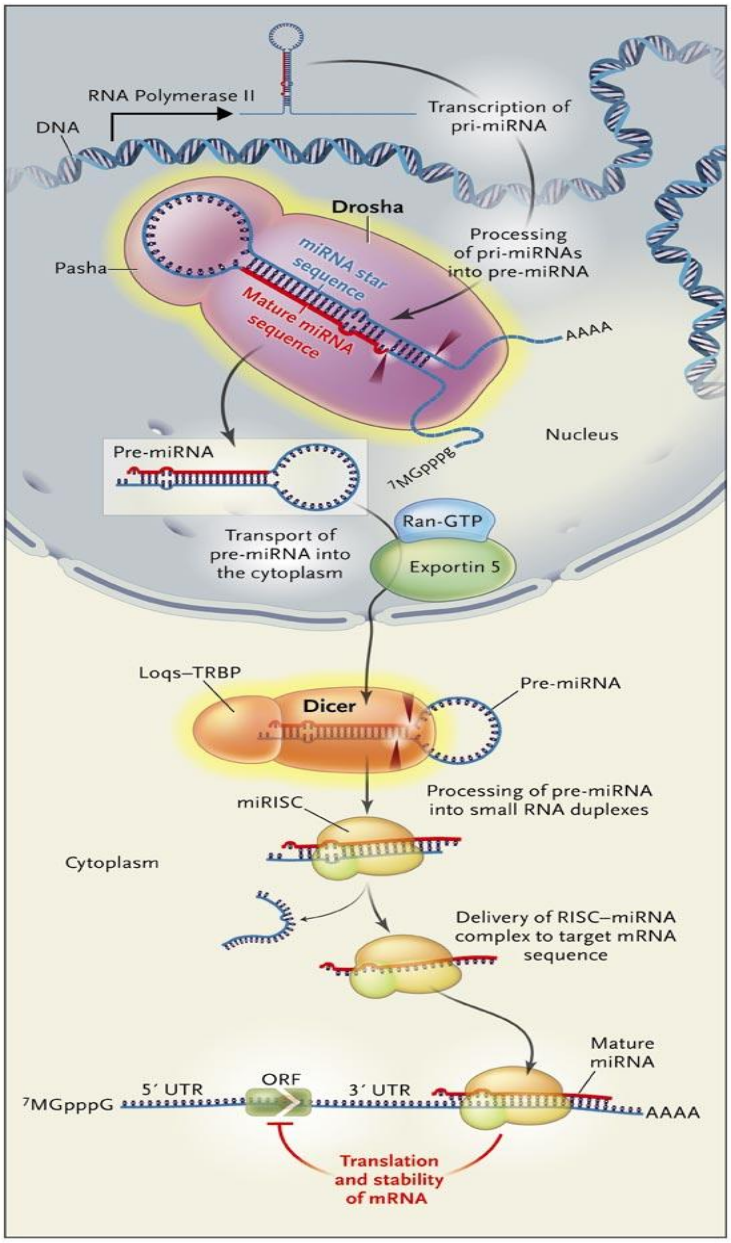

Figure 11. The overall representation of miRNA biogenesis from gene transcription to mRNAs targeting. Once transcribed by RNA Polymerase II, the primary transcript of ~ 1000 nt is processed by microprocessor complex Drosha/Pasha to pre-miRNA of ~ 80 nt. The pre-miRNA is transported by Exportin 5 from the nucleus into the cytoplasm, where it is processed by Dicer RNase to mature miRNA of ~ 22 nt. and loaded to the RISC complex. Within the RISC complex single-stranded ready-to-use miRNA is generated. Pairing of miRNA with 3' UTR of target mRNA promotes translation inhibition or degradation of mRNA.
(http://helicase.pbworks.com/w/page/17605642/Jonathan-Puza)

Until a few years ago miRNAs were considered only a translational regulators, however, recently a novel function has emerged: regulation of gene transcription. Through physical interaction with gene promoters, miRNA are able to mediate gene silencing by inducing heterochromatin formation at the promoter region of subsets of genes during cellular senescence [45], as well as activate gene transcription by binding to specific sites in the promoter [46]. Both mechanisms, either gene

silencing and gene transcription require also Ago proteins, and are currently under active investigation.

1.6. *Let-7* family of miRNAs

Let-7 miRNA (from ”lethal”) is one of the first identified miRNA. It was discovered as a heterochronic gene in *C.elegans* by forward genetics. During *C.elegans* development the seam cells, a particular type of hypodermal skin cells, undergo proliferation until larval stage 4. At the transition from larval stage 4 to adult, these cells stop dividing and undergo terminal differentiation. In worms with mutated *let-7* miRNA, the seam cells fail to exit cell cycle and to terminally differentiate, the resulting extra seam cell divisions lead to bursting of the vulva and death of the worm [47].

Further research on the *let-7* miRNA revealed a highly conserved miRNA family that is found in vertebrate, ascidian, hemichordate, mollusk, annelid and arthropod [48]. *Let-7* miRNAs are involved in many physiological as well as pathological processes, with a major role in induction of terminal differentiation and maintenance of the differentiated state. The human *let-7* family consists of the 12 members located on eight different chromosomes (Figure 12), the seed sequence is marked in red:

		Chromosome
Let-7a1	5'- UGAGGUAGUAGGUUGUAUAGUU -3'	9
Let-7a2	5'- UGAGGUAGUAGGUUGUAUAGUU -3'	11
Let-7a3	5'- UGAGGUAGUAGGUUGUAUAGUU -3'	22
Let-7b	5'- UGAGGUAGUAGGUUGUGUGGUU -3'	22
Let-7c	5'- UGAGGUAGUAGGUUGUAUGGUU -3'	21
Let-7d	5'- **A**GAGGUAGUAGGUUGCAUAGU -3'	9
Let-7e	5'- UGAGGUAG**G**AGGUUGUAUAGU -3'	19
Let-7f1	5'- UGAGGUAGUAGAUUGUAUAGUU -3'	9
Let-7f2	5'- UGAGGUAGUAGAUUGUAUAGUU -3'	X
Let-7g	5'- UGAGGUAGUAGUUUGUACAGU -3'	3
Let-7i	5'- UGAGGUAGUAGUUUGUGCUGU -3'	12
Mir-98	5’- UGAGGUAGUAAGUUGUAUUGUU -3’	X

Figure 12. let-7 miRNA family. Mature sequences of let-7 miRNAs are shown. (From MiRNAMap www.mirnamap.mbc.nctu.edu.tw)

The letters indicate different isoforms, while the number shows identical isoforms present in more than one genomic site (multiple copies). The isoform h is not present in humans, but exists in other species, like *Danio rerio*.

The high degree of sequence similarity suggests a functional redundancy, however different members might be regulated in a time-, tissue and/or cell-specific manner, since each isoform lies in

a different genetic context with its own promoter and cis-regulatory elements. It has been shown that the temporal regulation of let-7 is also conserved. Let-7 miRNA expression is first detected at late larval stages in *C. elegans* and *Drosophila melanogaster*, at 48 hours after fertilization in *Danio rerio*, and in adult stages of annelids and molluscs [48].

In human embryonic stem cells, the *let-7* miRNAs is not detectable, but becomes highly expressed upon differentiation [48]. This level remains high throughout life in adult differentiated tissues.

Let-7 miRNA plays an important role in cancer. Many let-7 target genes are associated with cell proliferation and cell cycle progression. Down-regulation of let-7 leads to the up-regulation of these genes. let-7 levels were found to be low in many primary tumors as well as in the cells obtained from distant metastasis. In many cancer types, down-regulation is associated with the EMT and its ectopic overexpression reduces chemoresistence, motility and invasiveness of cancer cells [49-51]. For this reason the potential therapeutic applications of this miRNA family have been evaluated [52]. Different studies performed *in vitro* and *in vivo* have shown that cancer cells in which let-7 was overexpressed, stopped growing or slowed down proliferation, reduced their motility and invasiveness, and increased sensitivity to chemotherapy [49, 53-55]. According a very recent study, the miRNA with decreased expression in patients with cancer most frequently associated with poor outcome is let-7 [56]. The best-studied key targets of let-7 miRNAs responsible for cancer cell aggressiveness and EMT are *HMGA2*, *RAS*, *CMYC*, *CCND1*, oncogenes that promote cell self-renewal and proliferation.

2. AIM OF THE STUDY

My project was focused on targeting MDA-MB-231 breast cancer cells with *let-7* miRNA and studying the effects of this targeting. The purpose of the research was to verify if and how ectopic overexpression of *let-7* miRNA in MDA-MB-231 cells is able to affect cell growth, cell cycle progression, differentiation and metabolism. Ultimately, the goal would be to use *let-7*mimics as miRNA replacement therapy.

3. ABSTRACT

miRNAs are short non-coding RNA that regulate gene expression at the post-transcriptional level by inhibiting the translation of mRNAs through pairing to their 3' UTR. The let-7 family of miRNAs regulates cell differentiation during embryogenesis and is responsible for the maintenance of the differentiated state in adult cells. Let-7 miRNA levels are often reduced in malignant tumors and its ectopic expression in cancer cells causes cell growth arrest, reduces invasiveness and down-regulates several oncogenes. To gain a further understanding of their biological functions, the breast cancer cell line MDA-MB-231 was transfected with let-7 miRNA mimics and their effect was examined by qPCR, western blot, flow cytometry and functional assays to determine stem cell characteristics and differentiation. We confirmed that let-7 miRNA mimics reduced cell proliferation, and HMGA2, Cyclin D1, Ras and Lin28A protein level in MDA-MB-231 cells. We found that let-7 miRNA down-regulated the levels of active β-catenin (ABC). We showed for the first time that let-7 miRNAs coordinately induce the enzymes in the serine biosynthesis pathway at the transcriptional level in MDA-MB-231 cells. Furthermore, we found that the protein level of the enzymes is differentially regulated: whereas the first two enzymes of the pathway are up-regulated, the last enzyme, phosphoserine phosphatase (PSPH), is down-regulated.

ABC down-regulation by let-7 mimics is consistent with the tumor suppressor role of let-7 miRNA family and represents an additional mechanism by which let-7 interferes with Wnt pathway.

The regulation of serine biosynthesis pathway is a novel and unexpected function of let-7 that raises many questions and leads to the exciting emerging field: Metaboloepigenetics.

4. MATERIALS AND METHODS

4.1. Cell line

The MDA-MB-231 cell line was obtained in 1973 from pleural metastatic effusion derived from a breast cancer patient [57, 58]. With fibroblast-like morphology, the MDA-MB-231 cells appear phenotypically as spindle shaped cells (Figure 13). *In vitro*, the MDA-MB-231 cell line has an invasive phenotype. It has abundant activity in both the Boyden chamber chemoinvasion and chemotaxis assays. The MDA-MB-231 cells are also able to grow in soft agar, an indicator of transformation and tumorigenicity, with a relatively high colony forming efficiency. *In vivo*, the MDA-MB-231 cells form mammary fat pad tumors in nude mice, while an injection of cells into the tail vein of nude mice has been shown to generate tumor colonies. MDA-MB-231 cells represent a model of triple-negative breast cancer: it does not express ER, PR or HER2.

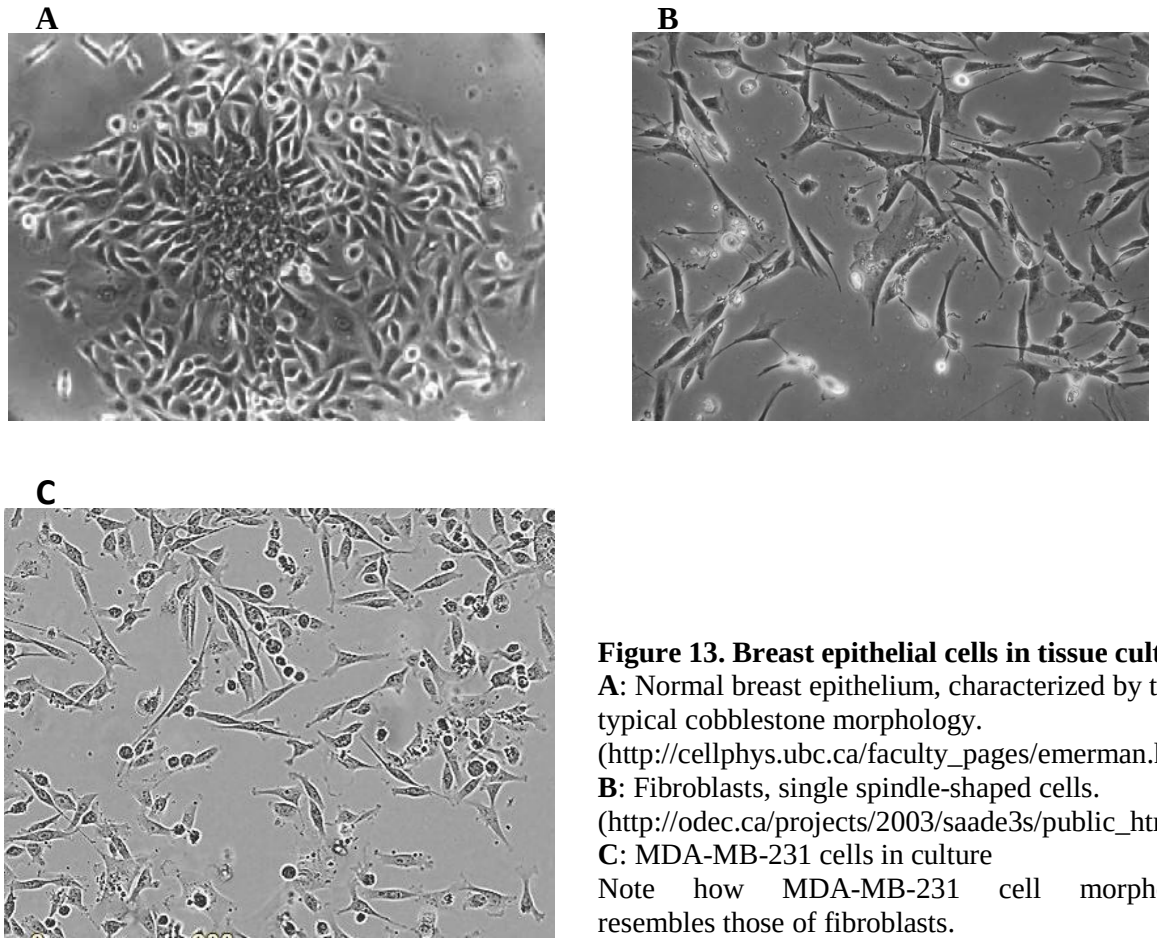

Figure 13. Breast epithelial cells in tissue culture.
A: Normal breast epithelium, characterized by the typical cobblestone morphology. (http://cellphys.ubc.ca/faculty_pages/emerman.html)
B: Fibroblasts, single spindle-shaped cells. (http://odec.ca/projects/2003/saade3s/public_html)
C: MDA-MB-231 cells in culture
Note how MDA-MB-231 cell morphology resembles those of fibroblasts.

4.2. Cell culture

MDA-MB-231 cells were maintained at 37ºC in 5% CO_2 in RPMI medium supplemented with 10% of fetal bovine serum (FBS), 1% of penicillin G and streptomycin sulfate (PS) and 1% of GlutaMAX (Invitrogen). Cells were passaged twice a week in order to keep the cell confluence between 15 and 80%. At reaching 80% confluence cells were washed with phosphate-buffered saline (PBS), detached by trypsinization and resuspended in the culture medium. RPMI, PS, FBS, Trypsin and PBS were provided by Lonza.

4.3. Lentivirus stable transfection

Stable ectopic expression of let-7 pre-miRNA in MDA-MB-231 cells was obtained using the commercial HIV-based Lentivector Expression System (SBI) encoding let-7 pre-miRNA or control siRNA. Four stably transfected cell lines were established: three expressing pre-miRNAs of let-7a, let-7b and let-7c isoforms, and one expressing shRNA targeting Firefly Luciferase. Each let-7 construct consisted of the stem loop structure and 300-500 base pairs of upstream and downstream flanking genomic sequences, that allows correct interaction with endogenous RNA processing machinery. All plasmids included also green fluorescence protein (GFP) under a different promoter, allowing us to isolate transfected cells by flow cytometry based on the green fluorescence (Figure 14). Transfection was performed according the producer's protocol for adherent cell lines. First, 293TN producer cells were transfected with packaging plasmid mix (SBI) in order to obtain pseudoviral particles carrying the whole construct to insert into the host cell genome. The supernatant containing pseudoviral particles was collected, mixed with Polybrene (final concentration 6 µg/ml), in order to neutralize the charge repulsion between virions and sialic acid on the cell surface [59], and added to 50% confluent MDA-MB-231 cells. The cells were incubated over night (ON), washed the next day and plated in the regular culture medium. The transfected cells were passaged seven times before being sorted by Fluorescence Activated Cell Sorting (FACS).

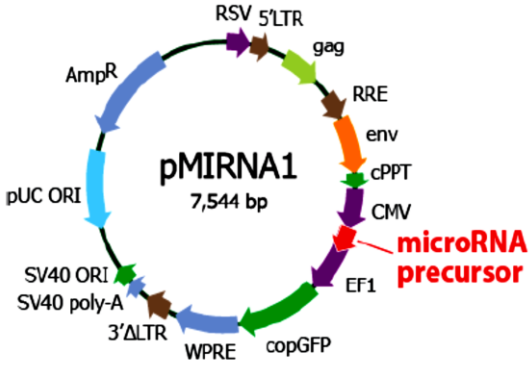

Figure 14. The map of plasmid used for lentiviral transfection. Pre-miRNA encoding sequence lies under the human cytomegalovirus (CMV) constitutive promoter. Gene encoding copepode GFP (copGFP) is under Elongation factor 1α (EF1) constitutive promoter. copGFP fluorescent marker allows to monitor and to sort cells positive for transfection.
5' and 3' Long terminal repeats (LTRs) allow to insert the construct into the genome. (from SBI)

4.4. Transient transfection

Transient transfection was performed using pre-miR miRNA Precursors (Ambion), that are small double-stranded RNA molecules which mimic endogenous mature miRNAs, and a lipidic transfection agent Interferin (PolyPLUS) according to the producer's protocol. 80.000 cells/well were seeded in a 12-well plate in RPMI medium supplemented with 5% FBS, 1% GlutaMAX and without antibiotic (1 ml of medium per well). When the cells have reached ~15% confluency, they were transfected with 15 pmol of Pre-miR miRNA Precursors using 8µl of interferin per well and incubated ON at 37°C. The next day after transfection (counted as day 1) the medium was changed in order to eliminate the excess of interefrin. At day 2 post transfection the cells were passaged to avoid too high confluence. The cells were harvested at the indicated in the producer's protocol time point (on day 3 or day 4 post transfection).

4.5. Cell growth estimation

Cell proliferation was monitored in the Incucyte (Essen Bioscience): a live cell imaging station consisting of an incubator and a microscope-scanner, that estimates cell confluence based on the phase-contrast image over time. Each well was scanned every 2 hours for 4 days from day 0 to day 4 post transfection. The growth curve was provided automatically by the Incucyte software. More than 3 biological replicates were obtained. In addition, cells were counted by a Countess™ automated cell counter (Invitrogen) at day 4. In order to distinguish between dead and live cells, the

cells were stained with Trypan Blue (Invitrogen) before counting (10 µl of cell culture mixed with 10 µl of Trypan Blue). Counting was performed in triplicates, and at least 3 biological replicates.

4.6. Apoptosis assay

The apoptosis assay used in this project is Caspase-activity based. On day 2 post transfection cells were seeded into a 96-well plate at approximately 10% confluency. Apoptosis reagent (Caspase-3/7 substrate, Essen Bioscence) was added to the medium at the dilution 1:2000. The Caspase-3/7 substrate is an inert, non-fluorescent substrate that freely crosses cell membranes, enters the cytosol, where it is cleaved by activated caspase-3 or -7. As a result, a green fluorescent dye is generated that labels DNA. Fluorescence was measured in the IncuCyte^{TM} by apoptotic object count or apoptotic object area estimation, normalized to image area. The cells were monitored over a period of two days (until day 4 post transfection). The assay was performed in triplicates on two biological replicates. Data were presented as fluorescent object counts per mm^2 over time.

4.7. Mammosphere formation assay

Cells were trypsinized and diluted to 3300 cells per 300 µl in Stem cell medium (supplied with (final concentrations): 20 ng/ml of basal fibroblast growth factor (bFGF; Invitrogen), 20ng/ml of epidermial growth factor (EGF; PeproTech) and 1X B27 (Life Technology), 1% of GlutaMAX (Invitrogen)). Assay medium was prepared by mixing 40 ml of MethoCult (Stemcell) with 60 ml of stem cell medium, and aliquoted. Cell suspension was mixed with 3 ml of assay medium and vortexed to obtain a homogenous mixture of cells. The cell mixture was then seeded in 24-well low adhesion plate (Greiner), 1 ml/well. Plate was incubated at 37°C for two weeks. Colonies were counted by automated gel counter (Oxford, Optronix Gelcount^{TM}), only colonies bigger that 50 µm were selected. The contrast was increased with 3-(4,5-dimethylthiazol-2-yl)-2,5-diphenyl tetrazolium bromide (MTT; Sigma-Aldrich) reagent that stains only live cells and thus allows to discriminate between living and dead cells. MTT was diluted in PBS to 1 mg/ml and 150µl were added to each well. The cells were incubated for 4h and then the medium was changed. The analysis was performed in triplicates.

4.8. Organoid assay

Trypsinized cells were diluted to 5000 cells per ml in RPMI medium containing 1X B27 (Invitrogen) and 20ng/ml EGF (Sigma). 80 µl of growth factor reduced matrix gel (BD Biosciences) were loaded in each well of 8-well glass chamber slide. Gel was left to solidify at 37°C for 20 min. Cell suspention was mixed 1:1 with assay medium (RPMI without serum, 5% matrigel and 20 ng/ml of EGF) and plated in matrigel coated 8-well chamber slide. The chamber slides were incubated at 37°C for one week. Colonies were analyzed on the microscope. The experiment was performed in triplicates.

4.9. Flow cytometry

Sorting. Stably transfected cells were trypsinized, resuspended in the 10% serum 1% L-Glu 1% penicillin/streptomycin DMEM and transferred into 15 ml tubes. Cells were sorted according to the GFP fluorescence. The sorting was performed twice, the first sort enriched the fluorescent cells from the total population and the second sort increased the purity of sorted fluorescent cells. Sorting was performed using FACSAria II flow cytometer (BD Biosciences).

Surface markers detection. The cells were washed in PBS, pelleted by centrifugation (1000 rpm per 5 min) and resuspended in staining buffer (PBS/2% FBS). The primary fluorophore-labeled antibody (Ab) against CD44 and CD24 were diluted (see Attachment 1) in PBS/2% FBS. The cells were incubated with Ab for 30 min at 4°C, then washed using staining buffer, pelleted by centrifugation and resuspended in 500 µl of staining buffer. 10000 cells were analysed. PBS and FBS were provided by Invitrogen.

4.10. Western blotting

Cells were washed with PBS and lysed directly in the plate using sodium dodecyl sulfate lysis buffer (3,2% sodium dodecyl sulfate (SDS), 13,8% Glycerol, 1% Tris, 7% beta-mercaptoethanol, 1% Triton, pH 6,8), scraped and transferred into an Eppendorf tube, boiled for 10 min at 95ºC and centrifuged at 13800g for 15 min. The supernatant was transferred in a new Eppendorf tube. The protein concentrations were determined by the Bio-Rad Protein Assay. 20 µg of protein per well were separated using 10% or 4-12% gradient NuPAGE Tris-Acetate gel (Invitrogen) in either MES or MOPs running buffer (Invitrogen) and transferred to 0,45 polyvinylidene fluoride (PVDF)

membrane (Millipore) previously activated in methanol. Blotted membranes were blocked in 5% nonfat dry milk in Tris Buffered Saline (TBS)-Tween solution for 1 hour at room temperature (RT) or ON at 4°C. Proteins of interest were detected by primary Ab (see Attachment N1 for nomenclature of Abs used) followed by the appropriate secondary Ab (anti-rabbit or anti-mouse (Dako)) diluted 1:5000 in 5% non-fat dry milk TBS-Tween buffer. The blots were incubated with primary Ab for 1 hour at RT or ON at 4°C, washed 3 times per 10 min with TBS-Tween buffer and incubated with secondary Ab for 1 hour at RT and washed again 3 times per 10 min. Antibody signals were visualized by chemiluminescence (SuperSignal West Dura, Pierce) and captured by charge-coupled device camera (Synoptic Group). Relative expression of the detected proteins to the α-actin or α-tubulin was quantified using a Gene Tools densitometry software (Synoptic Group).

4.11. Quantitative PCR (qPCR)

To generate total RNA lysates and cDNA, the Cell-to-Ct Kit (Ambion) was used. Approximately 100.000 cells were washed with PBS and lysed in 50µl of 1X Lysis Solution containing 0,5µl of DNase I, according to the producer's instruction. For cDNA generation, total RNA was reverse transcribed using random primers. 25 µl reaction contained 12,5 µl of RT buffer, 1,25µl RT enzyme mix, 2,5µl of total RNA lysate and was adjusted with 5,75µl of sterile dH_2O (B/Braun). The reverse transcription reaction was performed for 1h at 37°C, followed by 5 min at 90°C and, after termination, at 4°C. The cDNA was diluted with sterile dH_2O 1:10 before use.

To generate total miRNA cDNA, TaqMan miRNA Cell-to-Ct Kit (Ambion) was used. RT master mix for miRNA expression contained (per sample): 2 µl 10X RT buffer, 0,2 µl dNTP mix, 0,25 µl RNase inhibitor, 1,3 µl Multiscribe RT, 2 µl Pool 1 primers and 11,25 µl of water. 3 µl of lysate was added to the 17 µl aliquote of the master mix. The reverse transcription reaction was performed for 30 min at 16°C, 30 min at 42°C, followed by 5 min at 85°C and, after termination at 4°C.

For qPCR, 20 µl reaction per sample was prepared using 10µl of Gene expression solution (Ambion), 1 µl of primer mix (Applied Biosystems) and 4 µl of cDNA, the volume was adjusted with sterile H_2O. cDNA samples and "no-reverse transcription" controls underwent standard qRT-PCR amplification: 10 min at 95°C, (15 sec at 95°C, 1 min at 60°C) x 45 cycles. To analyze the relative expression of our gene of interest ,we used the ΔΔCt method (Bookout) with the endogenous internal control gene PGK, and the negative control siRNA treated sample as reference.

4.12. Fluorescence microscopy

Five thousand cells per well were seeded in a 8-well chamber slide. After 2 days cells were washed with PBS, fixed directly in the wells by incubation with formalin for 20 min at RT. The cells were subsequently washed 3 times with PBS, permeabilized with PBS/0,1% Triton X-100 5 min at RT, washed 3 times with PBS and blocked in PBS/10% FBS for 2 hours at RT. The cells were then incubated with the primary antibody for 2 hours at RT, washed 3 times with PBS/10% FBS and incubated for 1h at RT with primary Ab, washed 3 times with PBS/10%FBS and incubated for 30 min with fluorophore labelled secondary antibody (see Attachement 1). Cells were washed 3 times with PBS/10%FBS and the slide was mounted using ProLong Gold antifade reagent with DAPI (Invitrogen). The samples were analyzed using the Olympus 1X2-UCB fluorescence microscope.

5. RESULTS

5.1. Stable transfection was successful, but no effect of let-7 miRNA overexpression was observed.

In order to obtain MDA-MB-231 cell line stably overexpressing let-7 miRNA, the stable transfection was performed using HIV-based lentiviral vector encoding let-7 pre-miRNA.
The endogenous expression level of a, b, c, d, e and f let-7 miRNA isoforms in MDA-MB-231 cells was previously tested by qPCR (Figure 15) in order to evaluate which isoforms to choose for the transfection.

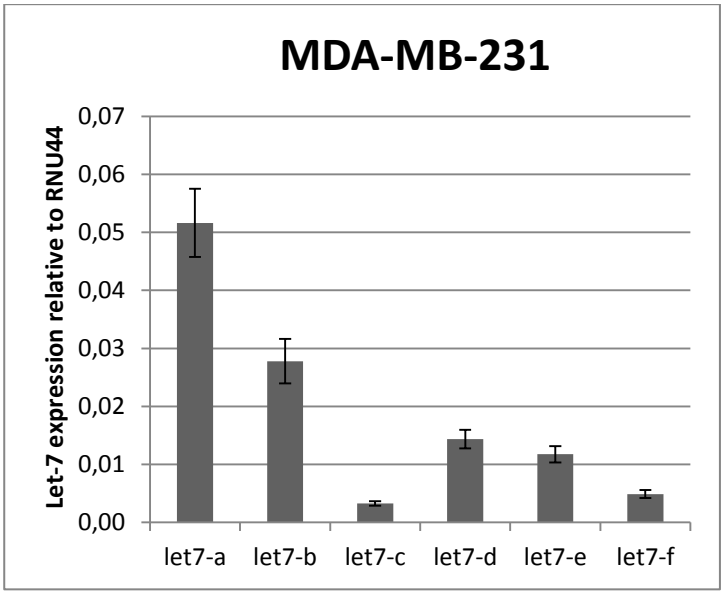

Figure 15. Expression of isoforms a, b, c, d, e and f of endogenous let-7 miRNA in MDA-MB-231 cells. Expression was normalized to the RNU44 gene. (From Munthe E., unpublished)

By comparing the expression of six isoforms, we found that *let-7a* was the highest expressed, *let-7c* isoform is expressed at a very low level, *let-7b* at an intermediate level, and the expression of let-*7d*, *-7e* and *-7f* is quite low. Based on these findings, we chose to generate cells with stable overexpression of *let-7a*, *let-7b* and *let-7c* isoforms, which represent the highest, the lowest and the intermediate endogenous *let-7* level. Lentiviral transfection was performed, and successfully transfected MDA-MB-231 cells were sorted by flow cytometry based on the green fluorescence produced by the product of *GFP* gene situated on the same plasmid. The control cells, transfected

with plasmid containing siRNA against Luciferase and copepod *GFP* (*copGFP*) gene-reporter, were sorted by flow cytometry as well. Two rounds of sorting generated a pure stably transfected cell population.

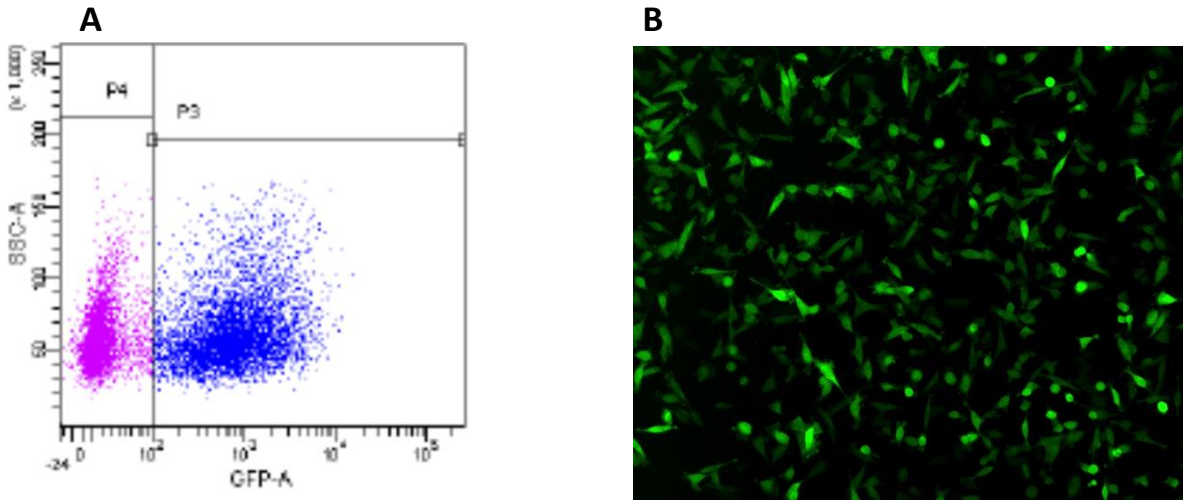

Figure 16. Cells transfected with *let-7c* pre-miRNA. A: The cell population P3 sorted by FACS based on the green fluorescence. **B:** GFP expression in sorted and expanded stably transfected cells. The picture is taken in the IncuCyte machine, 10X magnification, passage 2 after sorting.

The selection of positive cells based on *GFP* gene-reporter was successful, and very pure stably transfected cell lines were established (Figure 16). The fluorescence intensity per cell correlates to the number of copies of *GFP* gene inserted into genome, and thus should correlate with the number of pre-*let-7* copies per cell as they are in the same plasmid. For *let-7b* transfected cells, the sorted population was divided into two subpopulations: low intensity GFP and high intensity GFP fluorescence. We performed qPCR analysis to examine *let-7* expression in the stably transfected cells. We expected to detect overexpression of all three *let-7* isoforms compared to parental MDA-MB-231 non-transfected cells and Luciferase siRNA-transfected control cells. To our surprise qPCR showed very modest increase in the expression level of *let-7a* and *let-7b* (Figure 17). In addition, the expression level of *let-7b* miRNA did not correlate with the intensity of GFP fluorescence. However, we detected a 100-fold increase in the expression of the *let-7c* isoform, and we decided to carry on further experiments with this one. Probably, a and b isoforms expression did not increase in a relevant manner, because unlike isoform c, they have much higher basal level of expression in MDA-MB-231 cells.

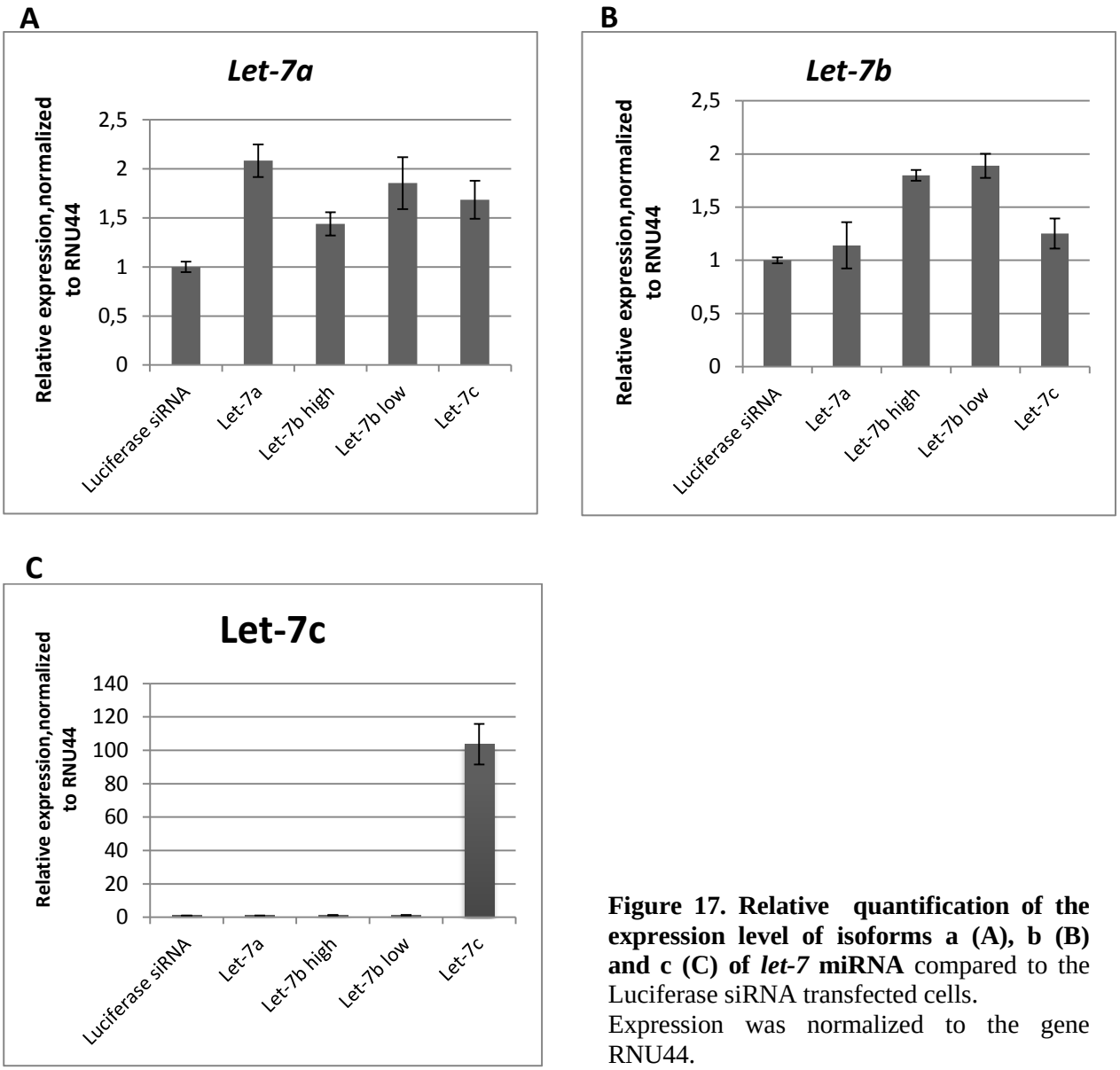

Figure 17. Relative quantification of the expression level of isoforms a (A), b (B) and c (C) of *let-7* miRNA compared to the Luciferase siRNA transfected cells.
Expression was normalized to the gene RNU44.

We initially wanted to assess the effect of *let-7c* overexpression on proliferation. Cell proliferation was estimated using the Incucyte. Untreated cells, cells transfected with siRNA against Luciferase or *let-7c* stably transfected cells were seeded in a 6-well plate and followed in the Incucyte for 5 days until they reached 100% of confluency (Figure 18).

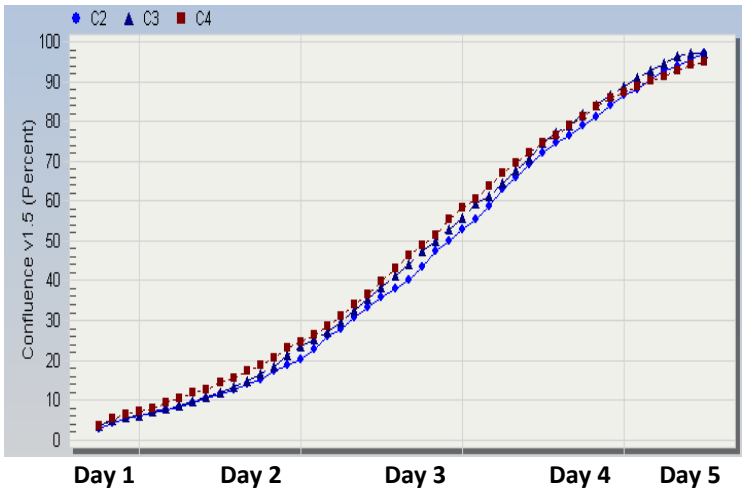

Figure 18. Growth curve of MDA-MB-231 transfected cells. Cell confluence of untreated cells (**C2**), siRNA Luciferase transfected cells (**C3**) and *let-7c* transfected cells (**C4**) at passage 7.

Unexpectedly, the growth curve showed no differences between the samples: strong overexpression of *let-7c* miRNA did not have any effect on the cell proliferation.

We performed Western Blot to see if the protein level of known targets of *let-7* miRNA, like HMGA2, cMyc, Ras and Lin28A, were altered in the *let-7c* overexpressing cells. Since miRNAs inhibit translation of mRNA of their target genes, we expected the protein level of all four genes to be reduced in *let-7c* transfected cells.

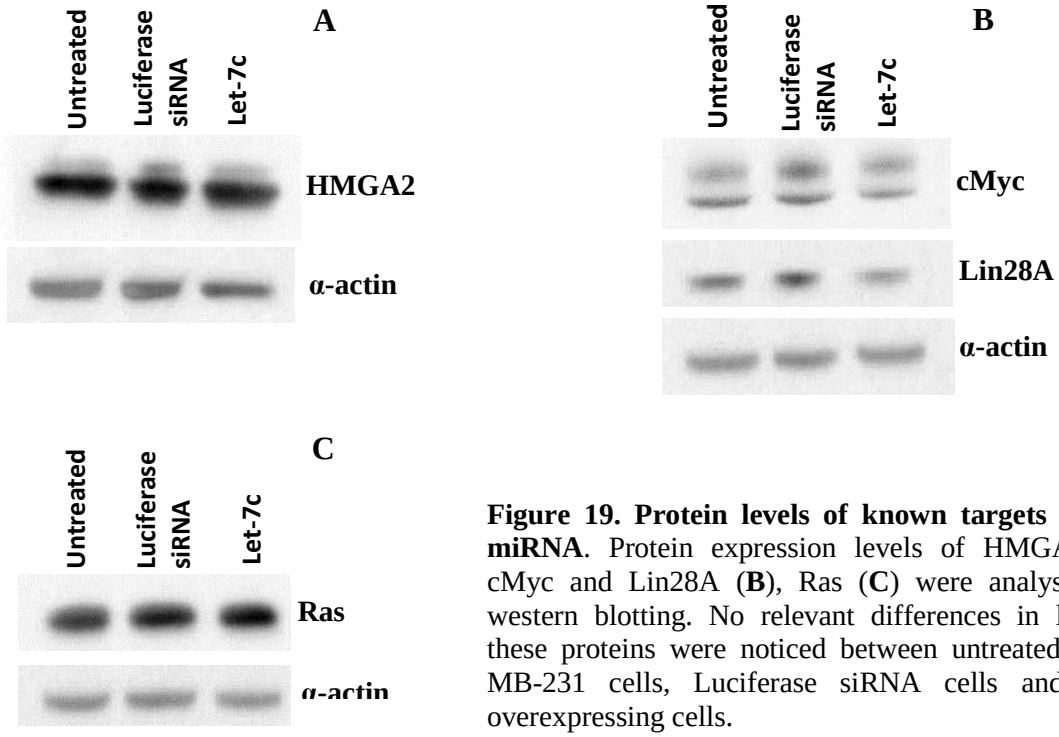

Figure 19. Protein levels of known targets of *let-7* miRNA. Protein expression levels of HMGA2 (**A**), cMyc and Lin28A (**B**), Ras (**C**) were analysed by western blotting. No relevant differences in level of these proteins were noticed between untreated MDA-MB-231 cells, Luciferase siRNA cells and *let-7c* overexpressing cells.

No differences in protein expression levels of neither of the let-7 target genes between controls

samples and *let-7c* transfected cells were observed. However, another two tests were performed on the *let-7c* transfected cells: the capacity to generate mammosphere and organoids. Mammosphere formation is considered to be a property of adult stem cells of breast tissue as well as a property of breast cancer stem cells [60]. As mentioned earlier, MDA-MB-231 is a mesenchymal-like breast cancer cell line, capable to grow in an anchorage-independent manner and forming mammospheres in three-dimensional culture. *let-7* has previously been shown to inhibit mammosphere formation in different breast cancer cell lines [61]. To investigate the mammosphere formation capacity of *let-7c* overexpressing cells, the cells were kept in 3D culture for 8 days and then the number and diameter of mammospheres were estimated using the gel counter. The test was performed in duplicates. Neither mammosphere number nor their diameter showed relevant differences between let-7c overexpressing and control samples (Figure 20).

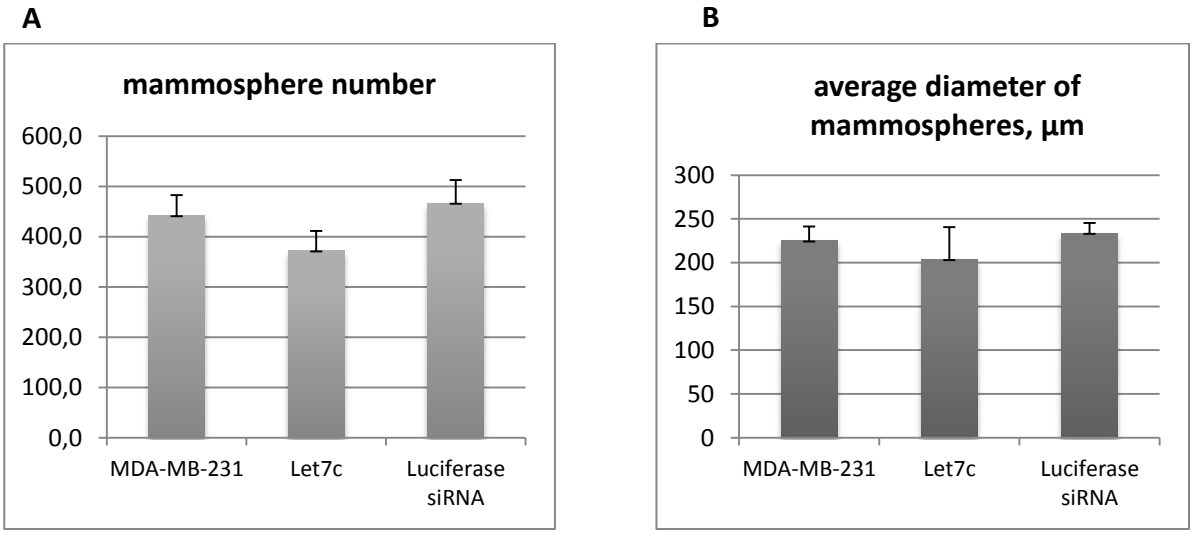

Figure 20. Mammosphere formation assay. No significant differences between samples neither in mammosphere number (**A**) nor in diameter of the mammospheres (**B**) were detected.

Organoid assay reveals the capacity of cells to form spherical organoids with protrusions in a 3-dimentional matrigel that mimics extracellular matrix, and thus to evaluate the presence of MMPs responsible for matrix degradation and invasiveness. As it is seen from Figure 21, no differences in organoid formation were observed between untreated cells, Luciferase siRNA cells and let-7c transfected cells, neither in number nor in the size or shape of organoids.

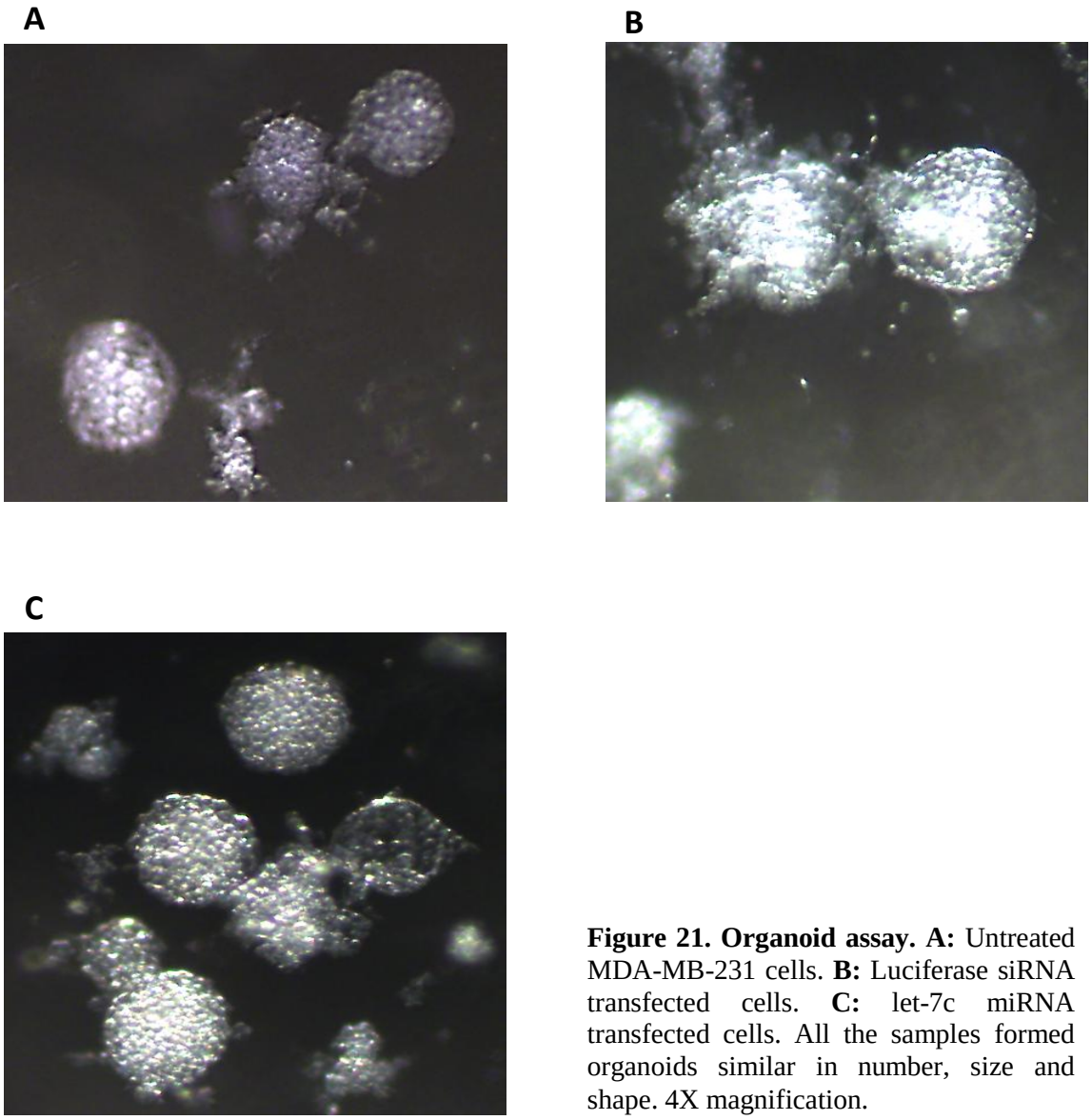

Figure 21. Organoid assay. A: Untreated MDA-MB-231 cells. **B:** Luciferase siRNA transfected cells. **C:** let-7c miRNA transfected cells. All the samples formed organoids similar in number, size and shape. 4X magnification.

In conclusion, despite a strong overexpression of *let-7c*, none of its functional effects was observed in our transfected cells. The manipulation of a biologic system could lead to unpredictable effects. According to the manual of producers, *let-7* primers pick up only mature form of *let-7* miRNA. We detect 100-fold increase of *let-7c* miRNA after transfection, so we can assume that the processing of precursor by Dicer, leading to the mature miRNA generation, occurs correctly. Since the goal of the project was to investigate the *let-7* miRNA biological effect on MDA-MB-231 cells, we decided not to dwell on the stable transfection and to proceed with the transient one.

5.2. Conditions of transient transfection of MDA-MB-231 cells with *let-7* mimics were optimized.

Transient transfection of MDA-MB-231 cells was performed using *let-7* Pre-miR miRNA precursors (hereafter called mimics) provided by Ambion. As a negative control, we used siRNA without any target (hereafter called negative control) or also cells treated with the transfection agent alone (hereafter called mock).

The first attempt of transient transfection was performed in 96-well plates following the transfection protocol provided by the manufacturer. The transfection was optimized with respect to interferin concentration, mimic concentration and cell number. We found that the transfection was optimal if the cells were transfected at 10 to 20% of confluency using amount of mimics and interferin recommended by the producer's protocol. We verified that interferin did not affect the cell proliferation rate significantly, showing low toxicity. As a positive control siRNA against Glyceraldehyde 3-phosphate dehydrogenase (GAPDH) was used. However, we did not routinely include this control. As GAPDH activity assay we used a fluorimetric GAPDH KDalert Kit (Ambion) (data not shown).

In order to get sufficient amounts of cells to perform different experiments, we optimized transfection for 24-well plates. All *let-7* isoform mimics were tested by growth estimation assay after transfection in 24-well plate. Let-7 transfected cells have displayed reduced proliferation compared to the negative control cells and mock. (Figure 22).

A

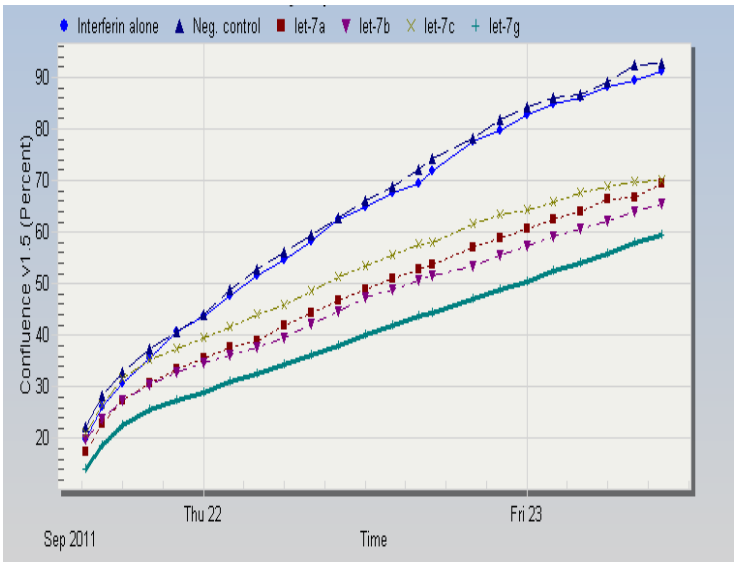

B

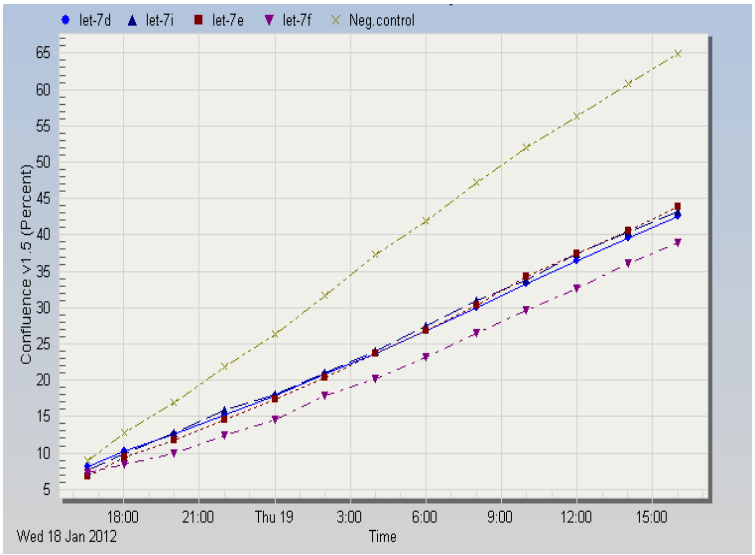

Figure 22. Proliferation assay. Cells were transfected in 24-well plate with let-7 mimics. **A:** isoforms a, b, c, g, negative control cells and cells treated with only transfection agent.
B: isoforms d, i, e, f and negative control. The cells were monitored in the Incucyte. The graphs show the cell confluence on day 4 and day 3 respectively.

In addition to the proliferation assay obtained from the Incucyte, total number of live cells were counted at the moment of harvesting at day 3 or day 4 post transfection, using automated cell counter and staining with Trypan blue (Figure 23). Number of let-7 transfected cells was lower than the number of negative control cells. No differences in the number of dead cells between samples were observed, indicating that the decrease in the cell number in let-7 treated samples is not caused by apoptosis. The counting was performed on three different biological replicates and confirmed the proliferation assay data obtained in the Incucyte.

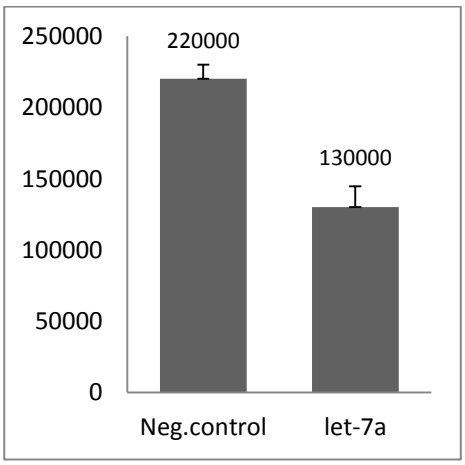

Figure 23. Cell count, cells/ml. The MDA-MB-231 cells were transfected with let-7a mimics and counted on day 3 post transfection. n=3. The difference in cell number between negative control and let-7a transfected cells is consistent with proliferation assay results based on Incucyte data.

5.3. *let-7* mimics down-regulate HMGA2, Ras, Lin28A and Cyclin D1.

To measure any functional effects of the *let-7* mimics, we checked the protein level of known let-7 targets like HMGA2, Ras, Lin28A and Cyclin D1 by western blot. The level of all four proteins was down-regulated in *let-7* transfected samples compared to negative control cells (Figure 24). Based on the band intensity, all *let-7* isoforms tested seem to down-regulate the target genes with similar efficiency.

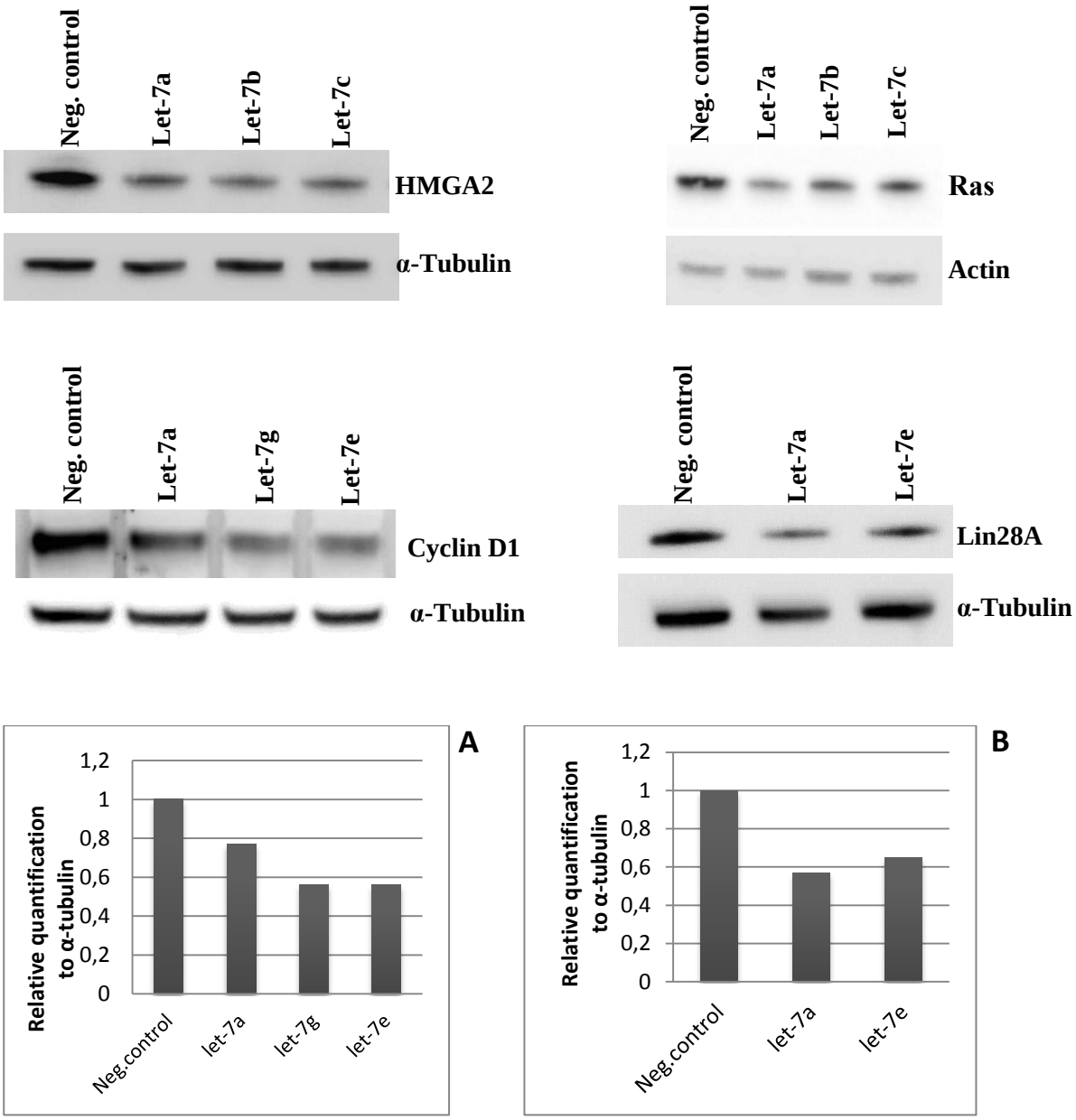

Figure 24. Detection by western blot of known targets of let-7 miRNA. In let-7 mimics transfected MDA-MB-231 cells the expression of all four genes (HMGA2, Ras, Lin28 and cyclin D1) is reduced at a protein level compared to the negative control cells. Densitometric quantification of cyclin D1 **(A)** and Lin28A **(B)** to α-tubulin.

5.4. Overexpression of *let-7* mimics does not cause apoptosis in MDA-MB-231 cells.

We assessed that *let-7* mimics reduce cell proliferation compared to the negative control cells. Furthermore, based on the cell counting, *let-7* did not seem to increase the cell death. However, we performed a control apoptosis assay based on Caspase-3 or -*7* activity detection. To include an additional control layer to the test, MDA-MB-231 cells were transfected with Glyceraldehyde-3-phosphate dehydrogenase (GAPDH) siRNA shown to induce apoptosis [62]. For this test, mimics of *let-7* isoforms a and e were used. The cells were followed in the Incucyte for 4 days. The data were analyzed using Object Counting program (Essenbio). No differences in apoptotic activity were observed between negative control and *let-7* treated samples. However, in the sample transfected with GAPDH siRNA an increase in number of apoptotic cells was detected (Figure 25). Apoptosis assay was performed in triplicates, on two biological replicates.

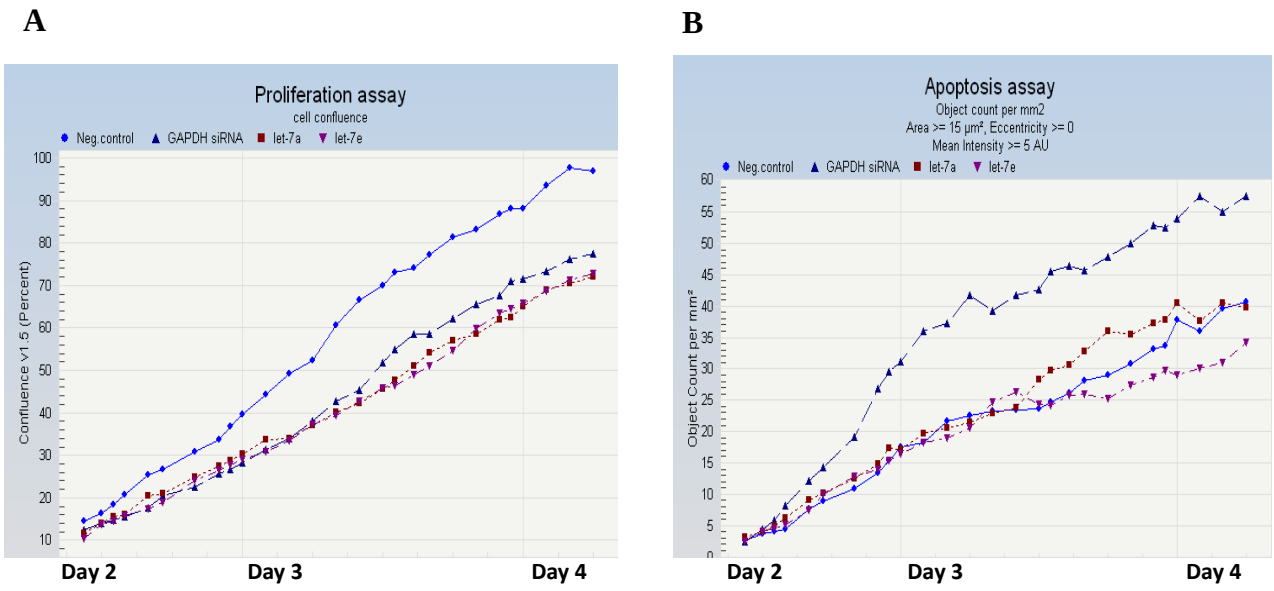

Figure 25. Apoptosis assay. MDA-MB-231 cells transfected with let-7 mimics and GAPDH siRNA. **A:** Proliferation assay. Compared to the negative control cells, let-7a, let-7e and GAPDH siRNA transfected cells show decrease in proliferation. **B:** Apoptotic activity. Only GAPDH siRNA transfected cells have an increased apoptotic activity respect other samples. Only one representative experiment is shown.

5.5. Histone 3 level is reduced in MDA-MB-231 cells upon *let-7* overexpression.

Since we have observed that, upon *let-7* treatment, the MDA-MB-231 cells slow down the proliferation, we wanted to have an additional evidence of the cell cycle deceleration. The Histone 3 (H3) expression is tightly regulated and is S-phase dependent. Thus, if the cell cycle is slowed down, H3 synthesis should be reduced as well. To verify that, H3 protein level was detected by western blot. We found that in *let-7* treated cells the level of H3 was reduced 50-80% compared to negative control cells (Figure 26).

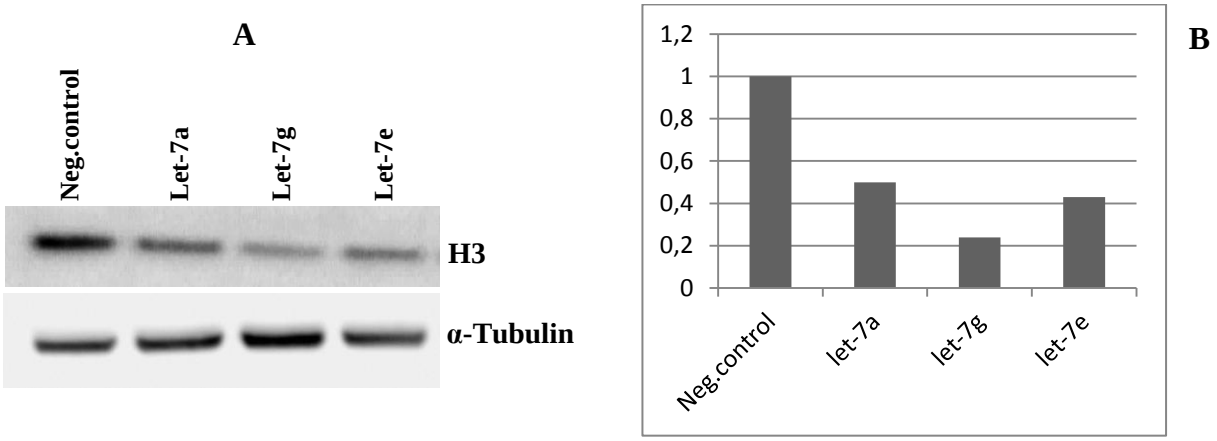

Figure 26. Detection of H3 by western blot. Cells were transfected with *let-7* mimics (isoforms a, g anf e), harvested on day 4 post transfection. Western blot was performed on total cell lysate. **A:** In all three *let-7* treated samples H3 level is reduced compared to the negative control cells **B:** The bands were quantified by densitometry analysis (Gene Tools) to α-tubulin. In let-7 treated cells H3 is reduced by 50-80% respect to the negative control.

5.6. Cell surface markers CD44 and CD24 were unchanged upon *let-7* overexpression.

CD44 and CD24 are cell membrane glycoproteins that are considered mesenchymal and epithelial markers, respectively. By using flow cytometry we determined the expression of these proteins on *let-7* treated or negative control cells to verify if the levels of CD44 and CD24 changes upon *let-7* transfection. Our analysis showed that *let-7*neither increased the level of CD24, nor decreased the expression of CD44 within the duration of transient transfection (3-4 days) (Figure 27).

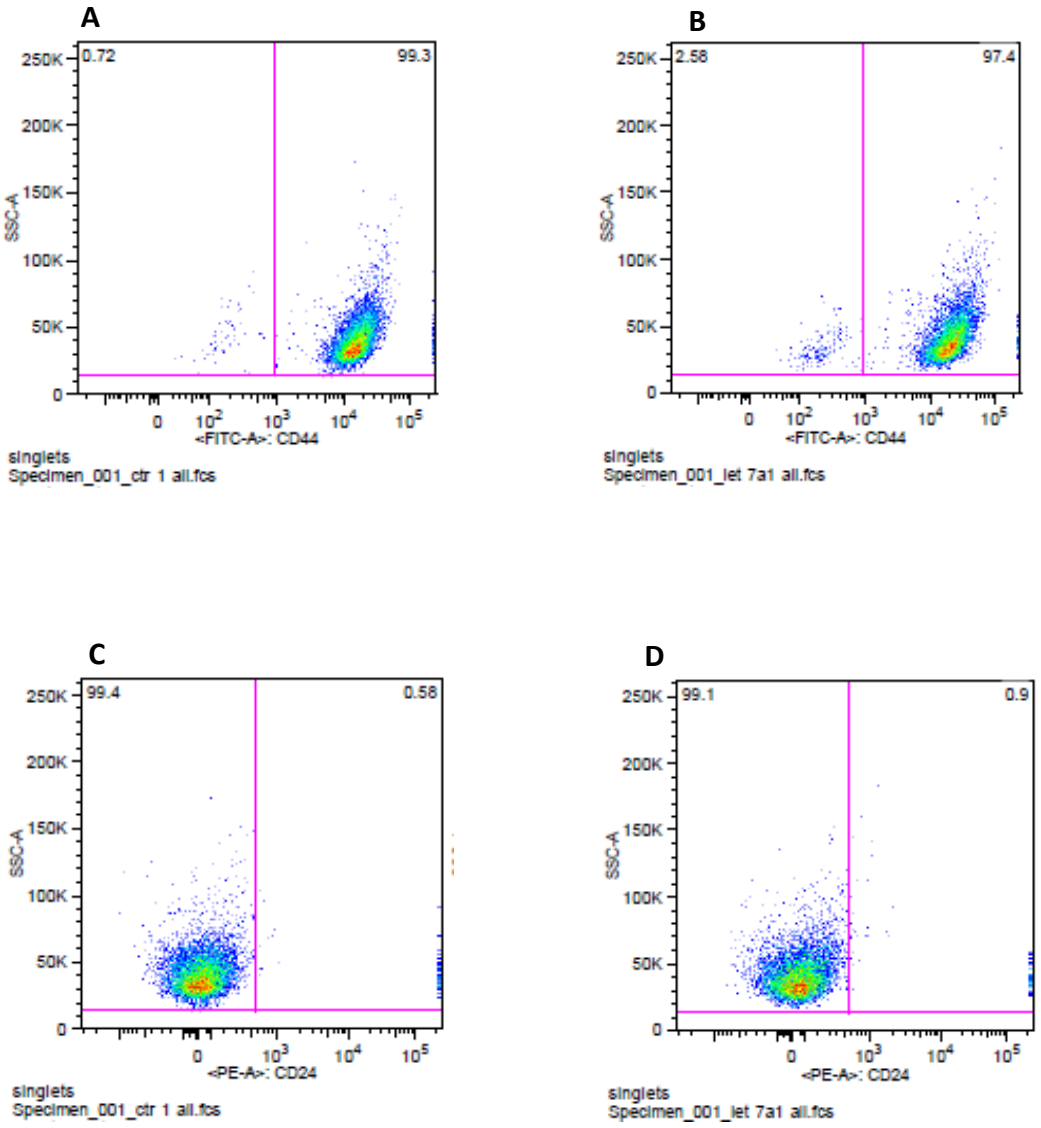

Figure 27. Expression of CD44 and CD24 in let-7 treated cells analysed by flow cytometry. Expression of mesenchymal marker CD44 in negative control (**A**) and let-7a transfected cells (**B**). Expression of epithelial marker CD24 in negative control **(C)** and let-7a transfected cells **(D)**. No differences were observed between samples.

In addition, we investigated if *let-7* was able to restore the expression of epithelial marker E-cadherin or down-regulate mesenchymal genes *SNAIL* and N-cadherin. All three genes were found to be expressed below the qPCR detection level (data not shown).

5.7. β-catenin is de-activated upon *let-7* overexpression.

β-catenin is a key protein of the canonical Wnt signaling pathway that often is activated in tumors. Wnt pathway is active in MDA-MB-231 cells and β-catenin is activated. Furthermore, due to the absence of adherence junctions in this cell line, all β-catenin is localized in the cytoplasm. We wanted to see if tumor suppressor *let-7* miRNA can affect its post-translational modifications.
Cells were transfected with *let-7e* mimics, harvested on day 3 post transfection and active β-Catenin (ABC) was detected by western blot using an antibody which specifically recognizes β-Catenin dephosphorylated on Ser37 or Thr41 (Figure 28).

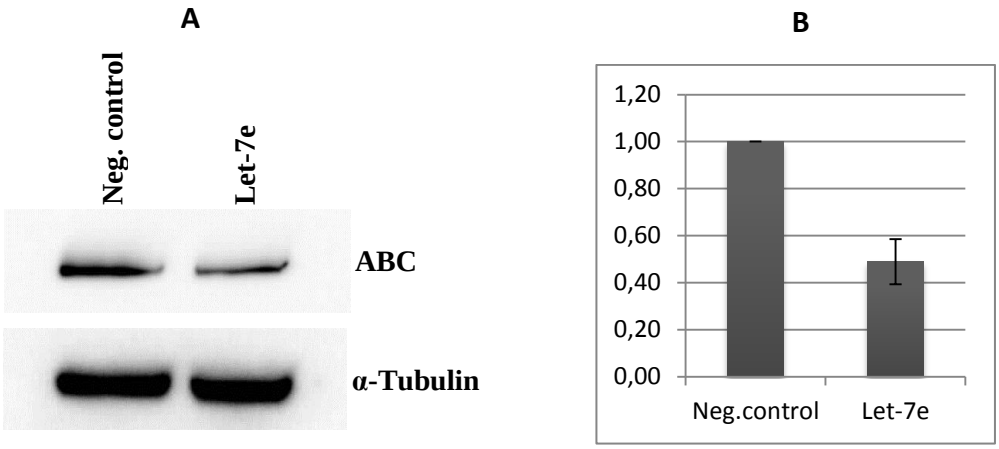

Figure 28. **Western blot analysis of ABC**. MDA-MB-231 cells were transfected with *let-7e* mimic and ABC was detected on day 3 post transfection. **A:** protein level of ABC in *let-7e* sample is reduced compared to the negative control **B:** Densitometric quantification shows 40-60% reduction in ABC level (quantified to α-tubulin). Data were expressed as mean ± SD (n = 3).

Total β-Catenin protein level was also examined by western blotting on day 2, 3 and 4 post transfection. Interestingly, total β-catenin protein levels were increased in *let-7* treated samples compared to the negative control siRNA treated cells. Furthermore, it increased from day 2 to day 4 post transfection (Figure 29).

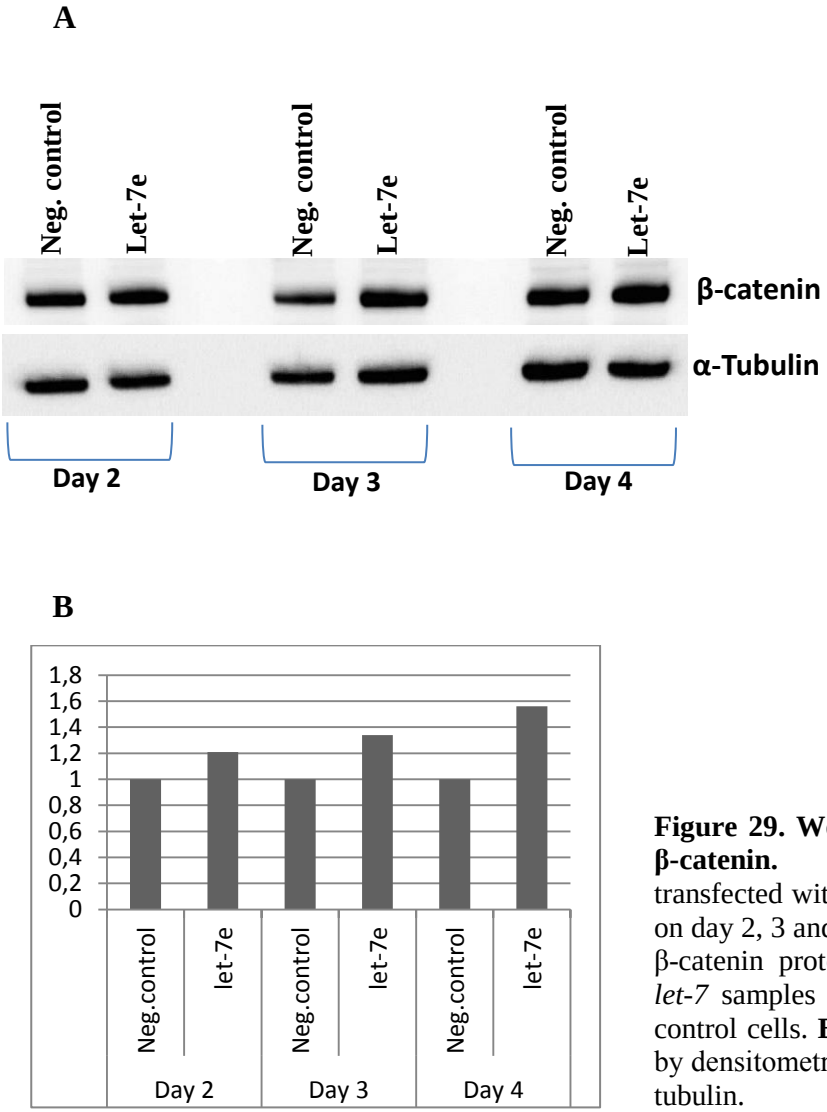

Figure 29. Western blot analysis of total β-catenin. MDA-MB-231 cells were transfected with *let-7e* mimic and harvested on day 2, 3 and 4 post transfection. **A:** Total β-catenin protein level is increased in all *let-7* samples with respect to the negative control cells. **B:** The bands were quantified by densitometry analysis (Gene Tools) to α-tubulin.

Total β-catenin was also detected by immunofluorescence in negative control and *let-7* transfected cells to observe its subcellular distribution. β-catenin, shown in green (Figure 28), is mostly present in the cytosol with apparently higher concentration in the perinuclear space. In contrast, it does not seem to localize to the cytoplasmic membrane. No observable difference in intensity of fluorescence was seen between negative control and *let-7* treated cells. To compare the β-catenin subcellular localization to normal epithelial cells, an image of gastric epithelial cells at the fluorescence microscope is also reported (Figure 30).

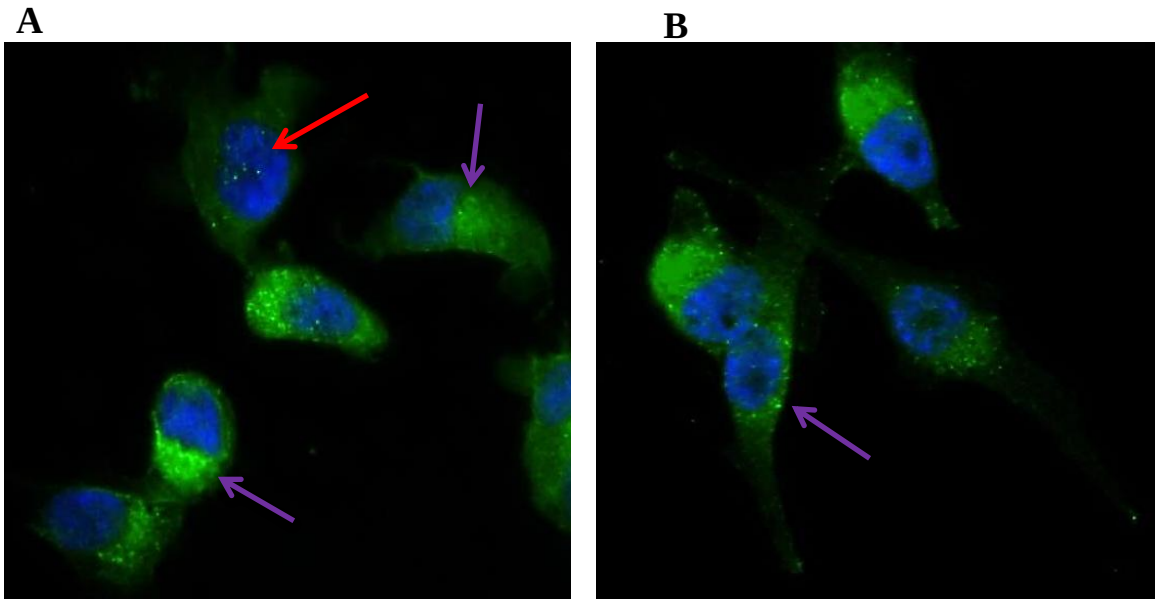

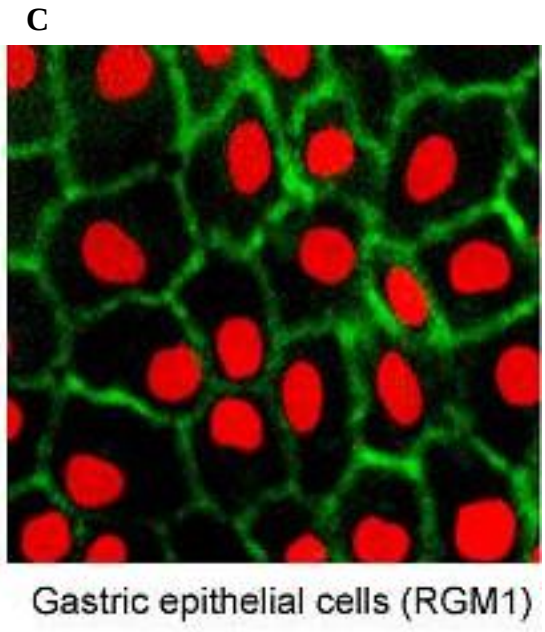

Figure 30. Detection of total β-catenin by immunofluorescence in MDA-MB-231 cells.
A: Negative control cells. β-Catenin is expressed throughout cytoplasm and appears to be concentrated in perinuclear spaces (violet arrows), boundaries are undefined due to the loss of β-Catenin from the adherence junction (in this cell line most of elements of adherence junctions are lost). β-Catenin might also localize in the nucleus (red arrow). In this case it would be a portion of total β-Catenin constituted by ABC.
B: Let-7 treated cells. β-Catenin shows the same intensity and localization as in the negative control cells. Nuclei stained with DAPI (blue).
C: Localization of β-Catenin in normal gastric epithelial cells. β-Catenin staining marks the boundaries of the cell membrane, showing that it localizes predominantly to adherence junctions in the plasma membrane. Very little β-Catenin is observed in the cytosol (nuclei stained with propidium iodide (red). http://www.abcam.com/beta-Catenin-antibody-ab2365.html#beta-Catenin-Primary-antibodies-ab2365-9.jpg.)

5.8. The expression of components of the serine biosynthesis pathway is altered upon *let-7* overexpression in MDA-MB-231 cells.

Recently, it was shown that the flux through serine biosynthesis pathway is increased in some aggressive triple-negative breast cancers, and protein levels of the first enzyme of this pathway, phosphoglycerate dehydrogenase (PHGDH) are elevated in 70% of estrogen receptor (ER)-negative breast cancers [63]. Phosphoserine aminotransferase 1 (PSAT1) is found to be up-regulated in different cancers and associated with increased cell proliferation and aggressiveness [64-66]. Since the *let-7* miRNA family is well documented tumor suppressor, we wanted to investigate whether it could have an impact on the expression of serine pathway enzymes in the MDA-MB-231 triple-negative breast cancer cell line.

Serine biosynthesis occurs in the cytoplasm and consists of three consecutive reactions catalyzed by PHGDH, PSAT1 and phosphoserine phosphatase (PSPH) (Figure 31).

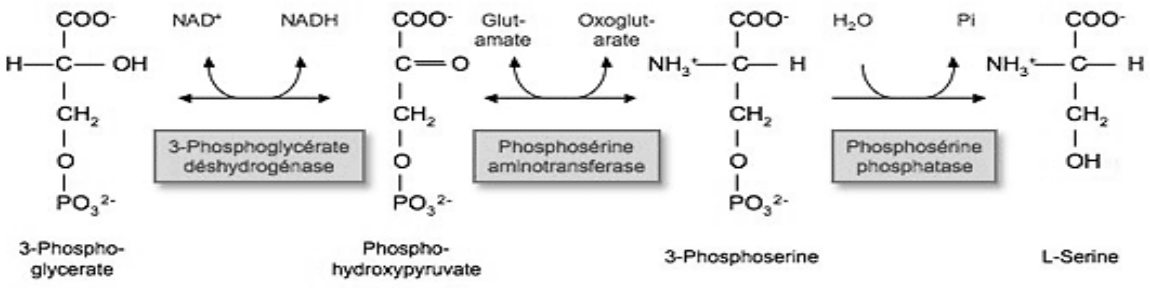

Figure 31. Serine pathway. The pathway consists of three steps. In the first step PHGDH oxidizes 3-phosphoglycerate to 3-phosphohydroxypyruvate. In the second step PSAT1 deaminates 3-phosphopiruvate to produce 3-phosphoserine. The last step is catalyzed by PSPH that dephosphorylates 3-phosphoserine to L-serine. Under high biosynthetic flux, the pathway is controlled by the last step through mechanism of end product inhibition.

Expression of all three enzymes of the serine pathway, PHGDH, PSAT1 and PSPH, was measured by qPCR at day 3 and/or 4 post transfection using *let-7a*, *-7c* and *-7g* mimics (n=4). Surprisingly, qPCR analysis revealed that in *let-7* transfected cells, all three enzymes are up-regulated. The highest increase in expression was always observed in *PHGDH*, the first enzyme of pathway (Figure 32).

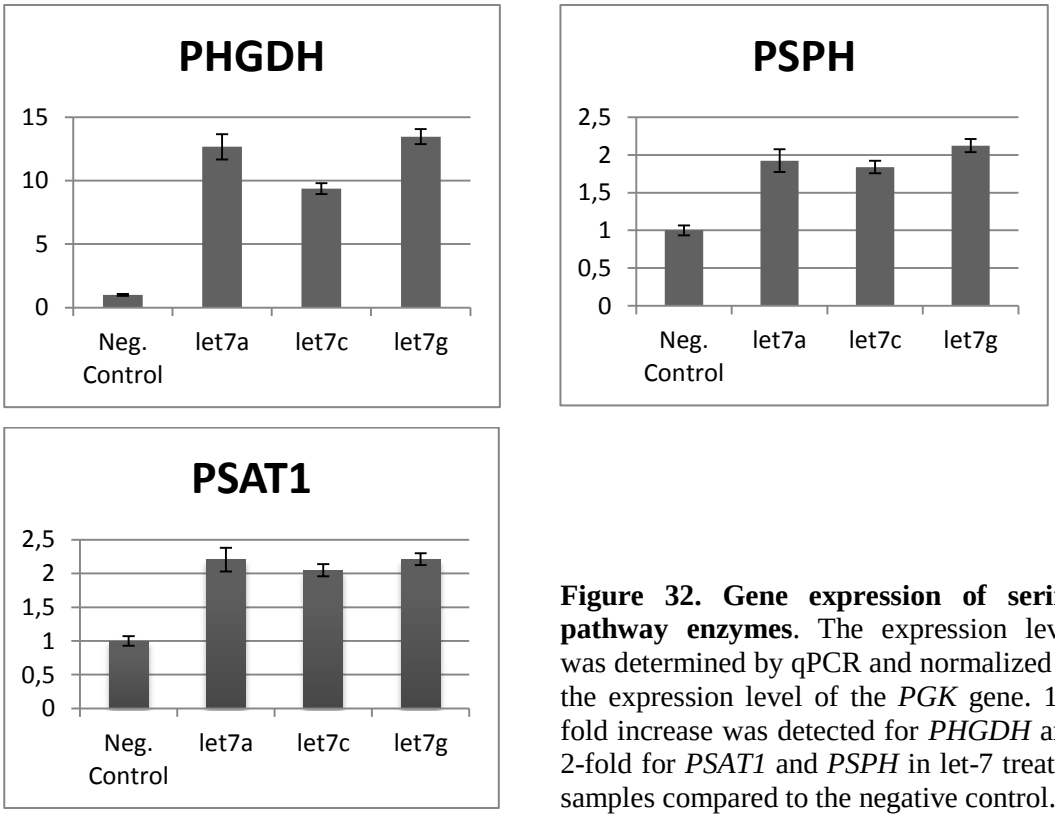

Figure 32. Gene expression of serine pathway enzymes. The expression level was determined by qPCR and normalized to the expression level of the *PGK* gene. 10-fold increase was detected for *PHGDH* and 2-fold for *PSAT1* and *PSPH* in let-7 treated samples compared to the negative control.

Subsequently, the protein level of all three enzymes was determined by western blot and quantified by densitometry. Cell were transfected with *let-7* isoforms a, b, c and g. Interestingly, while PHGDH and PSAT1 showed increased protein levels in *let-7* transfected cells, the last enzyme of serine pathway, PSPH was down-regulated at the protein level in all *let-7* tested samples. α-tubulin was used as loading control (Figure 33a and b).

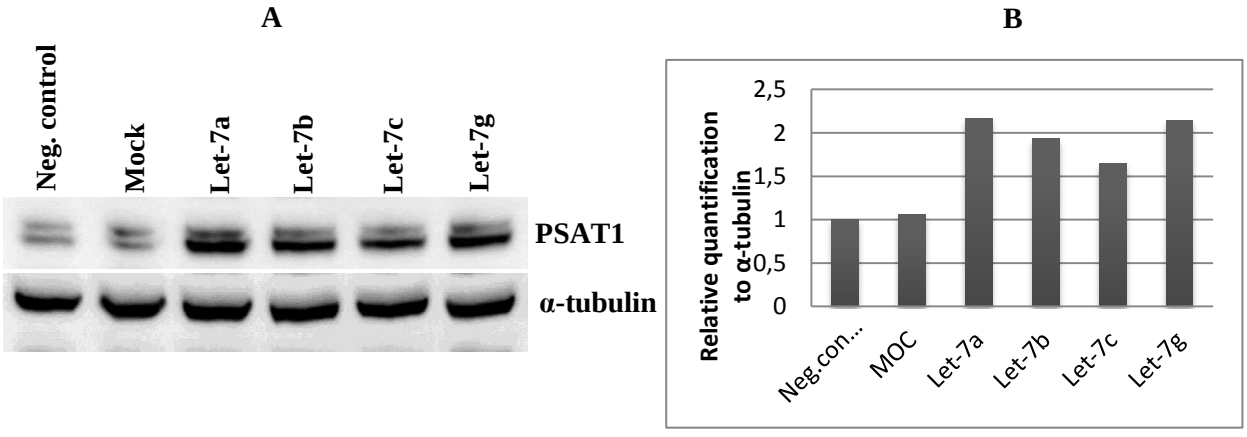

Figure 33a. Protein level of serine pathway enzymes. A: in MDA-MB-231 cells transfected with let-7 mimics (isoforms a, b, c and g) PSAT1 is increased compared to the negative control and mock. **B:** the bands were quantified to α-tubulin by densitometry analysis using Gene Tools software. Compared to the negative control and mock, PSAT1 level is increased up to 2-fold in all let-7 treated samples.

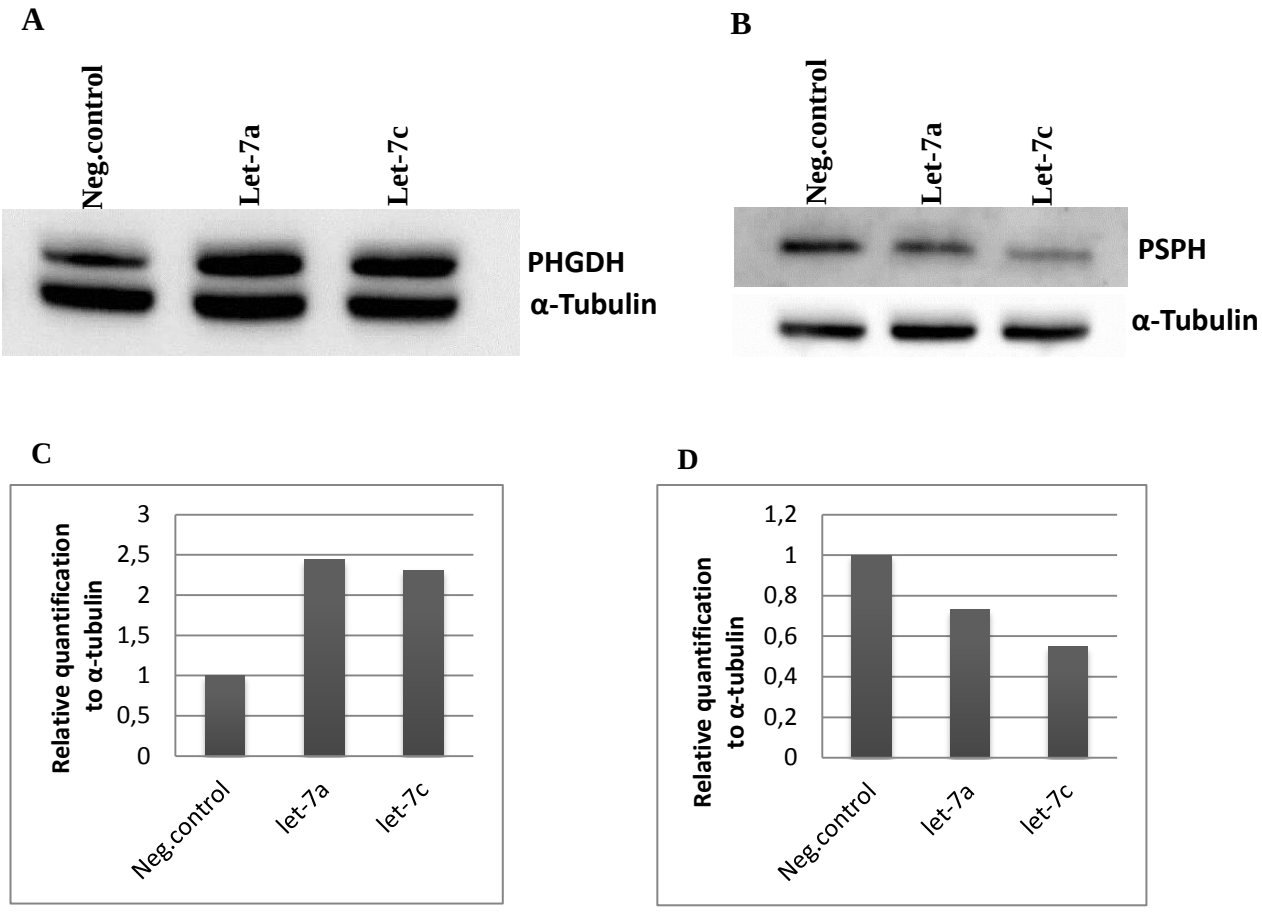

Figure 33b. Protein levels of serine pathway enzymes. A: western blot analysis shows the detection of PHGDH in the MDA-MB-231 cells transfected with let-7 mimics (isoforms a and c).
B: detection of PSPH level in the MDA-MB-231 let-7 transfected cells (isoforms a and c).
C and D: quantification of the bands to α-tubulin by densitometry analysis using Gene Tools software. PHGDH level in the let-7 treated cells is increased more than 2-fold with respect to the negative control. PSPH level is reduced up to 50% in let-7 treated cells compared to the negative control cells. α-tubulin is used as loading control.

5.9. The serine synthesis pathway is altered upon induction of adipose differentiation in immortalized mesenchymal stroma cells.

Let-7 miRNA is known to mediate differentiation, so we wondered if the increase in serine pathway enzymes upon *let-7* transfection could be linked to the initiation of the differentiation. For this purpose, in collaboration with a member of our group Magne Skårn, the expression level of serine pathway enzymes was tested by microarray in iMSC#3 mesenchymal stroma cells induced to differentiate. It have been found that both genes, *PHGDH* and *PSAT1*, were up-regulated upon induction of adipogenesis, while *PSPH* remained unchanged (Figure 34).

A

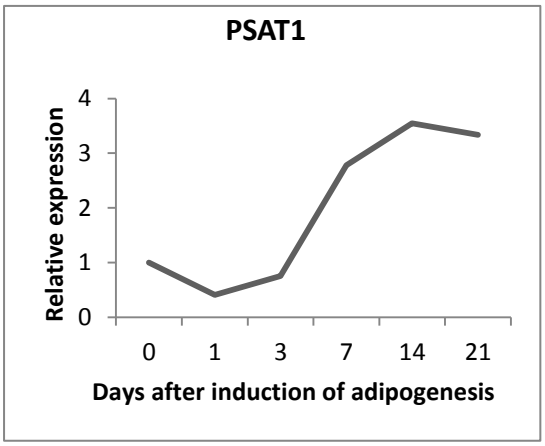

B

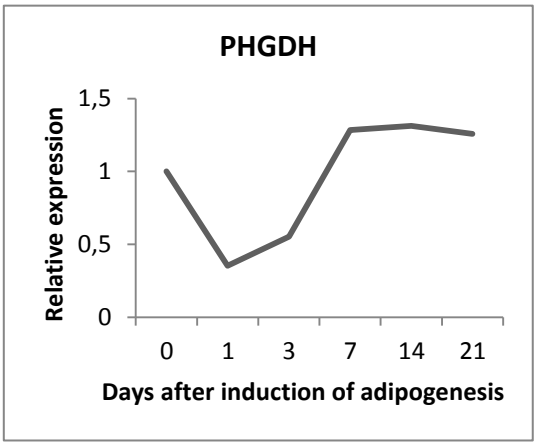

C

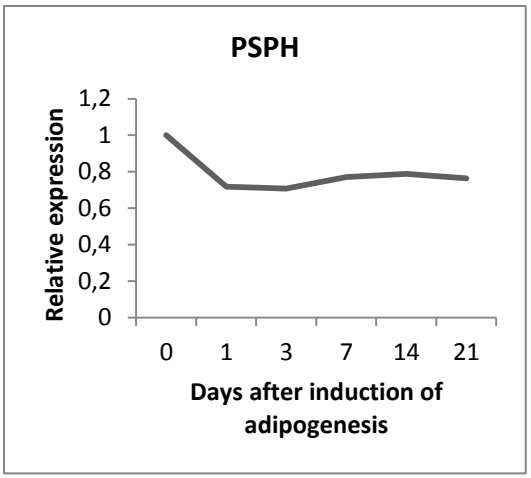

Figure 34. Expression level of serine pathway enzymes. Immediately after administration of differentiation mix, the expression level of all three enzymes decrease, but from day 1 *PSAT1* (**A**) and *PHGDH* (**B**) expression level starts to rise up and this increase persists for several days (up to 13 days in *PSAT1* and to 6 days in *PHGDH*), while the *PSPH* (**C**) expression level remains constant. Microarray data. (From M. Skårn).

In addition to the measuring of the expression level of *PHGDH*, *PSAT1* and *PSPH* also the cell proliferation was estimated by MTS assay. As it is expected during terminal differentiation, iMSC#3 cells stopped to proliferate upon adipose differentiation induction (Figure 35.)

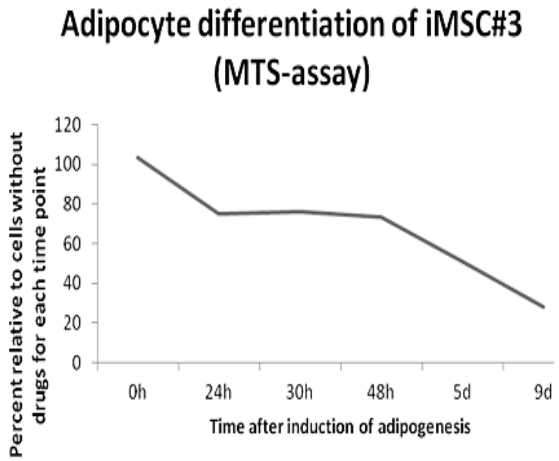

Figure 35. Proliferation assay. Upon induction of adipogenesis iMSC#3 cells enter cell cycle arrest and stop proliferating. (From M. Skårn).

Furthermore, the expression of let-7 miRNAs in the iMSC#3 cells upon adipocyte differentiation was investigated. Two isoforms, let-7g and let-7d were found to be induced and increased their level from day 3 to day 14 post differentiation induction (Figure 36).

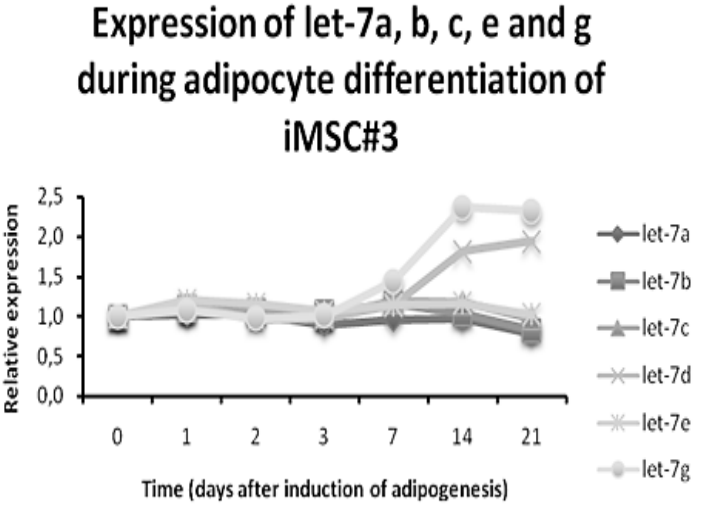

Figure 36. Relative expression of let-7 miRNAs. iMSC# cells induced to differentiate into adipocytes. The expression of let-7d and let-7g is increased from day 3 to day 1 of induction of differentiation. (Data from M.Skårn)

6. DISCUSSION

Let-7 miRNAs constitute a highly conserved family that target mRNAs of genes involved in cell proliferation, cell cycle progression, angiogenesis and cell migration, like *RAS* GTP-ase, *CMYC*, *CCND1* and *HMGA2* [67-69]. Furthermore, *let-7* levels are often reduced in cancers and its ectopic expression reduces cancer cell growth and aggressiveness [50, 51]. Therefore, *let-7* miRNA is considered as a potential therapeutic agent. Also, there should be limited toxicity of *let-7* ectopic expression, since it is present in all adult differentiated cells.

First, we established three MDA-MB-231 cell lines with stable overexpression of *let-7* miRNAs. We used three different *let-7* isoforms: a, b and c. To exclude any unspecific effect due to the presence of the plasmids, we used siRNA against Luciferase as a control. All four constructs had also GFP gene under a separate promoter to enable selection of transfected cells.

The construct carrying the pre-miRNA gene and the GFP gene with respective promoters was integrated into the genome, as indicated by the green fluorescence detected by microscope after several passages. After being passaged 7 times, the cells were sorted by FACS, and the GFP positive cells were expanded. The expression level of *let-7* miRNAs in the *let-7* stably transfected cell lines was tested by qPCR, but among the three isoforms, only *let-7c* transfected cells showed a strong increase of expression above the endogenous level. In untreated MDA-MB-231 cells, according to the qPCR data (see Figure 13), *let-7a* and *let-7b* isoforms are expressed at much higher level than the *let-7c*, and this could at least partly explain their small increase after stable transfection. Unexpectedly, no phenotype was observed in the *let-7c* overexpressing cells, neither in the cell proliferation nor in the protein level of known *let-7* targets. According to the producer's datasheet (Ambion), the *let-7* primers used for qPCR should only detect mature *let-7* miRNA, excluding that the miRNA transcription or maturation was impaired. However, between the generation of the mature double-stranded miRNA and the formation of the active regulatory complex there is an additional step, where miRNA is unwind and delivered to the RISC by the RISC loading complex (RLS). In RLS, after the unwinding, strand selection occurs, one strand is degraded and the another one is loaded to the catalytic core of the RNAi machinery [42]. If these steps do not occur correctly, the translational inhibition might be compromised. So, one possible explanation could be that the mature miRNA was not correctly loaded to the RISC complex and, therefore, no translational inhibition of target mRNAs occurred. Another possibility is that the expression level of let-7 miRNA obtained by stable transfection just was not high enough. An

alternative hypothesis, that the endogenous let-7 level was already sufficient for full inhibition of target genes is highly unlikely, since by the transient transfection a good reduction was obtained.

In the second attempt to overexpress *let-7* miRNA in MDA-MB-231 cells, we used transient transfection with mature miRNA mimics, which was successful. We confirmed that known *let-7* targets HMGA2, Ras, Lin28A and Cyclin D1 were down-regulated upon treatment with *let-7* mimics in the triple-negative breast cancer MDA-MB-231 cell line. We also found that *let-7* overexpression reduced the proliferation of MDA-MB-231 cells. We observed that H3 was down-regulated in the *let-7* transfected cells with respect to the negative control cells. The transcription of H3 is known to be S-phase dependent, thus these data are consistent with the overall picture that has emerged upon *let-7* treatment: decrease of cell proliferation, down-regulation of cell cycle associated genes like Cyclin D1 and HMGA2. All together these data suggest that *let-7* transfected cells undergo slowdown of cell cycle. In fact, it has been shown that *let-7* overexpression causes accumulation of cells in G1 cell cycle phase in primary fibroblasts [70].

The study of EMT process is complicated by the fact that EMT in cancer cells is often incomplete, can be transient, and is influenced by the microenvironment that is absent in *in vitro* conditions.
MDA-MB-231 cells have a mesenchymal-like phenotype and as a first check for an eventual reversion back to the epithelial phenotype, we looked at the morphology. We did not observe any morphological sign of MET. The expression of epithelial marker E-cadherin was not restored, nor could we observe any reduction in the mesenchymal marker CD44 or increase in the epithelial marker CD24. However, we cannot exclude that a prolonged exposure to the *let-7* overexpression might induce MET. Despite evident advantages of transient transfection like simplicity and rapidity of the method, it has some limitations. The most relevant one is the transient nature, excluding the possibility to perform functional assays that require more than 5-6 days, like mammosphere colony formation or generation of organoids. However, this problem could be at least partly overcome by the re-transfection.

We tested different *let-7* isoforms to evaluate if there is any functional difference between them. However, no relevant differences between examined isoforms were observed: all tested isoforms reduced the MDA-MB-231 cell proliferation and the protein level of target genes with similar efficiency. Each isoform is coded by genes on different chromosomes, so it might be that *in vivo* the main difference between single isoforms is determined by their genetic context. In addition, different isoforms might have different degree of complementarity for the same genes with consequent variation in translational inhibition efficiency.

β-catenin

β-catenin is a bifunctional protein that in differentiated epithelial tissues forms, together with E-cadherin and α-catenin, cell-cell adherence junctions. In addition, there is a small cytoplasmic fraction of β-catenin, that is constitutively targeted for proteasomal degradation. Upon Wnt signal, β-catenin is stabilized and translocated to the nucleus where it acts as a transcriptional coactivator for Wnt target genes. *Let-7* was discovered as a heterochronic gene that mediates larval to adult transition in seam cells in *C. Elegans*. Interesting, Wnt/β-catenin pathway is also involved in development and cell fate specification of seam cells in *C. Elegans* [71]. However, while the Wnt pathway sustains asymmetric division of seam stem cells, *let-7* promotes their terminal differentiation resulting in proliferation arrest. Therefore, *let-7* counteracts the Wnt/β-catenin function. *Let-7* miRNAs are known to down-regulate some of β-catenin's target genes, i.e. *CCND1* and *CMYC*, through binding to the 3' UTR of their mRNAs. However, to date, there is no evidence in the literature of a direct effect of *let-7* on the β-catenin expression or its post-translational modifications. The specific down-regulation of ABC by *let-7* miRNA found here extends the role of *let-7* in the regulation of the Wnt signaling pathway. Nevertheless, the observation that *let-7* reduces the level of ABC does not reveal the mechanism by which this occurs. This mechanism is undoubtedly indirect since *let-7* miRNA cannot affect phosphorylation by itself. One possibility is that *let-7* somehow regulates the activity of the degradation complex or affects signal transduction. For example, one of the key components of the degradation complex, GSK-3β, is inactivated when phosphorylated on the Ser 9 residue through PI3K/Akt pathway [72]. Let-7 has been shown to down-regulate several components of the insulin-PI3K-mTOR pathway, among which Akt2 [73]. In conclusion, down-regulation of ABC by *let-7* is a novel function of this miRNA and needs to be fully investigated. In this sense, global gene expression profiling or proteomics could be helpful to identify which genes among those regulated by let-7 might cause the ABC reduction.

We also found a weak, but progressive increase in the total β-catenin level in *let-7* transfected cells. In normal epithelial cells, the majority of β-catenin is localized to the cell membrane where it is bound to E-cadherin to form the adherence junctions. E-cadherin is not expressed in MDA-MB-231 cells, therefore all β-catenin localizes in the cytoplasm or nucleus. Furthermore, the Wnt pathway is active in this cell line, suggesting that β-catenin is stabilized and active. It would be reasonable to expect that *let-7* miRNA could restore, for instance, β-catenin proteasomal degradation that occurs in normal epithelial cells. The increase in total β-catenin raises a question: which fraction of β-catenin increases after *let-7* transfection? Normally, phosphorylated β-catenin is targeted for

proteasomal degradation and is rapidly degraded. The higher level of total β-catenin found in *let-7* samples implies either decreased degradation or increased synthesis. Interestingly, in a metastatic SKBR3 breast cancer cell line, treatment with retinoic acid increased the total β-catenin level by increasing its stability, and increased its recruitment to the cell membrane [74]. We did not detect increase of cell membrane localization of β-catenin in our cell line, nor could we show a re-expression of E-cadherin. It could be that prolonged exposure to *let-7* mimics would give a different outcome.

Serine pathway

During this work, a considerable finding was made concerning the serine biosynthesis pathway enzymes PHGDH, PSAT1 and PSPH. Several studies have linked the up-regulation of these enzymes to cancer progression and aggressiveness. It has been shown that PSAT1 increases chemoresistance in colon cancer and that its down-regulation is associated with a favorable clinical outcome in recurrent breast cancer, while the *PHGDH* gene is amplified in some breast cancer cell lines. In fact, this pathway has a prominent role in cell proliferation: it provides not only building blocks for protein synthesis, but also precursors for glycine and cysteine, carbon for purines and pyrimidines as well as precursors for structural components of biological membranes like phospholipids and sphingolipids. It is not surprising that actively proliferating cells require increased serine production. At the same time, it is logical to expect that cells slowing down the proliferation or entering cell cycle arrest do not need to produce continuously new building blocks. So that some studies has even considered PSAT1, as well as PHGDH, as a novel target for cancer therapy [66]. PSAT1 previously had been found reduced upon HMGA2 siRNA transfection in MDA-MB-231 cells by Else Munthe. We wanted to see if *let-7* miRNA was able to down-regulate (directly or indirectly) the serine pathway enzymes in MDA-MB-231 cells as well, as it was reasonable to expect from a tumor-suppressor miRNA, thought to stop or decrease cell proliferation. Thus, all three serine pathway enzymes were detected by qPCR and by western blot. The result was surprising and required a reconsideration of the role of the serine pathway in the cell fate: cells transfected with *let-7* mimics had a reduced proliferation, but at the same time, had higher PHGDH, PSAT1 and PSPH level. Thus, our data were not consistent with serine pathway biological function, as described above.

Thorough literature search revealed at least two cases where increased expression of PSAT1 did not correlate with cell proliferation and/or DNA replication. The first example relates to the cold-

induced white to brown adipocyte transdifferentiation in mouse [75]. When mice are exposed to cold (6 degrees C for 10 days), brown adipocytes arise in white adipose tissue (WAT) through a direct transdifferentiation process. The direct transdifferentiation occurs without increase in cell number. Furthermore, the expression of the gene coding for C/EBPalpha (an antimitotic protein) in WAT upon cold exposure, was increased. Among genes up-regulated in WAT during transdifferentiation, the researchers found *PSAT1*, which up-regulation dynamic they defined as surprising: *PSAT1* expression was induced up to 3-fold on day 1 and day 3, but then reverted to its basal level on day 6. In the second example, *PSAT1* was found to be up-regulated during terminal differentiation of epidermal keratinocytes, where *PSAT1* mRNA amount increased on day 1 after induction of differentiation, reached the maximum level (3-fold) on day 3, and then started to decrease again, remaining however well above the basal level of expression [76]. Interestingly, we also detected a similar dynamic pattern in the *PSAT1* and *PHGDH* expression in iMCS#3 mesenchymal stem cells induced to differentiate into adipocytes. Except the same day of induction of differentiation, when the level of *PSAT1* and *PHGDH* slightly dropped, from the day 1 their level progressively increased up to 3 fold after two weeks (see Figure 32), while the cells stopped to proliferate (see Figure 33) and *let-7g* and *let-7d* miRNA expression has started to increase (see Figure 34). But even more interesting is that the expression pattern of all three serine pathway enzymes in iMCS#3 cells was very similar to those detected at a protein level in MDA-MB-231 cells: PHGDH and PSAT1 were up-regulated, while PSPH was unchanged or down-regulated (in our case).

An important conclusion from all these data is that an increase of serine pathway activity in the absence of cell proliferation might be associated with ongoing differentiation process.

Let-7, as it has been underlined many times, promotes differentiation. Could regulation of the enzymes in the serine pathway be somehow involved in mediating the differentiation process?

To date, there is no explanation in the literature regarding the functional role of PSAT1 or PHGDH in differentiation. However, there is evidence that increased levels of the final product of the serine pathway, L-serine, may be irrelevant for cell metabolism, when exogenous serine is available. First, intracellular L-serine is in equilibrium with extracellular serine, and, furthermore, knock down of the last enzyme of pathway, PSPH strongly diminishes cell proliferation and cyclin D1 levels in cutaneous squamous cell carcinoma even in the presence of high level of exogenous L-serine [63, 77]. All these data suggest that serine synthesis pathway might play an additional role in cell fate, beside the serine biosynthesis.

Evidence that serine production may not be the only important function of this pathway comes also from a metabolite study using isotopically labeled molecules. This study revealed that, upon

PHGDH suppression, the metabolite in the serine pathway with the largest reduction was the α-ketoglutarate (αKG), whereas intracellular serine level was not changed [63]. Furthermore, suppression of PSAT1 also caused a significant reduction in the aKG level. According to this study, the serine synthesis pathway is responsible for approximately 50% of the net conversion of glutamate into aKG in the cell.

In this perspective, regulation of the serine pathway enzymes acquires a special significance.

Another fundamental study and model of serine biosynthesis pathway is to be considered. The activities of the enzymes in the serine pathway are low in the rat liver [78]. However, the enzymes can be induced by hormonal or dietary manipulation *in vivo* [79]. When the rat is fed with a low-protein diet, all enzymes in the serine pathway are induced. Interestingly, there is a strong induction of PSAT1 and PHGDH (20 and 12-fold respectively), but only a 2-fold induction of PSPH. This causes a change in the metabolite ratios, with an increase in phosphoserine (P-Ser) concentration respect to those of serine (Figure 35).

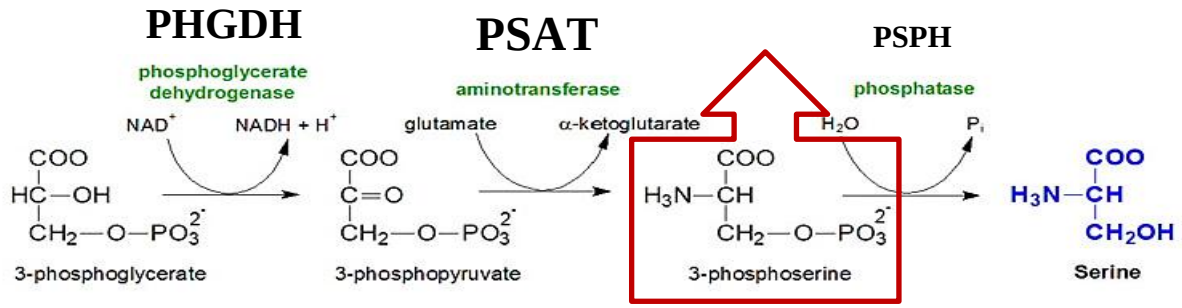

Figure 37. The distribution of the intermediates of the serine synthesis pathway changes upon low-protein diet in rat. The disequilibrium in the pathway is moved to the L-phosphoserine phosphatase step. The P-Ser concentration increases. The size of the letters in the names of enzymes have been chosen in relation to their relative amount in the cell. The picture is adapted from http://themedicalbiochemistrypage.org/amino-acid-metabolism.php.

The most relevant consequence of these changes is the appearance in the tissue of P-Ser that is undetectable in normal-diet fed rat (<0,01 µmol of P-Ser per/g liver in normal diet vs 0,255 µmol of P-Ser/g liver in low-protein diet).

Two major metabolites have been revealed by the studies performed on the serine biosynthesis pathways mentioned above: α-KG and P-Ser. Our system is far from the *in vivo* rat liver, however, we cannot exclude that induction of the serine pathway by *let-7* miRNA might produce a similar effect also *in vitro*, in our breast cancer cell line. From this point of view, it becomes very relevant the differential expression pattern of serine pathway enzymes upon *let-7* transfection and, even

more, the fact that the last enzyme of pathway, PSPH, seems to be regulated differently at the transcriptional level versus the translational level in our model system. As for the diet-induced changes in rat liver, *let-7* overexpression creates analogous changes in the enzyme levels: PHGDH and PSAT1 are up-regulated, while PSPH is down-regulated at a protein level. Importantly, the reduced PSPH level in MDA-MB-231 cells cannot be attributed to the mechanism of end-product inhibition by which serine pathway is regulated. Product inhibition occurs through the competitive binding of the product to the catalytic site of the enzyme and thus affects only enzymatic activity and not the protein level. Of interest, we found that the *PSPH* (mRNA) is predicted to have a *miR-200* binding site in the 3' UTR (TargetScanHuman 6.1). This binding site is conserved across species. *miR-200* is a miRNA found to be lost in mesenchymal-like breast cancer cell lines and is able to inhibit EMT and cell motility [80, 81].

Considering the similarity of enzyme amount distribution with the samples reported above, it would be tempting to speculate that the P-Ser level and α-KG might be increased after *let-7* treatment.

Could these two metabolites have a role apart the metabolic one? And, if so, what could this biologic role be?

The first consideration leads us to look towards a new and rapidly expanding field: METABOLOEPIGENETICS. This exiting field links energy metabolism to the epigenetic control of gene expression crucial for many processes, among which cell differentiation. The metabolites are found to be essential cofactors for enzymes that mediates epigenetic changes, like DNA methyltransferases, DNA demethylases, histone methylases and histone demethylases as well as histone acetyltransferases and histone deacetylases [82]. Of interest is that metabolites from the tricarboxylic acid cycle (TCA) or the serine biosynthesis pathway, in particular, α-KG is an essential cofactor of histone demethylases of the Jumonji C domain (JMJD) family and the TET family that mediates DNA demethylation.

In addition to the serine pathway, cells have two other pathways to produce α-KG: from glutamate, catalyzed by Glutamate dehydrogenase and from isocitrate, catalyzed by Isocitrate dehydrogenase (IDH). There are two isoforms of IDH, cytoplasmic IDH1 and mitochondrial IDH2, both are shown to be mutated in > 75% of gliomas and ~ 20% of myeloid leukemias [83-85]. Interestingly, mutated IDH generates 2-hydroxyglutarate (2-HG) instead of α-KG, and it has been shown that 2-HG inhibits the activity of the α-KG-dependent dioxygenases (like histone JMJD and the TET family enzymes). This inhibition leads to a genome-wide histone and DNA methylation alterations [84]. These evidences raise another important question: are small variations of intracellular α-KG levels able to affect demethylase activity? The first step to answer these questions is to measure the metabolite concentrations in cells transfected with *let-7* mimics and compare it with negative

control cells. It could be obtained, for example, by commercial Kits (Biovision) or by nuclear magnetic resonance. In fact, we have initiated a collaboration with S.Wilson at the Chemistry Department at UIO to measure α-KG and other metabolites levels. In addition to the α-KG level, the JMJD activity can be measured as well, using commercially available kits, like The JMJD2C Chemiluminescent Assay Kit (BPS, Bioscience).
Another evidence of the importance of α-KG in cancer comes from two studies which showed that α-KG inhibits the proliferation of colon adenocarcinoma cell lines [86] and inhibits tumor growth and angiogenesis in lung carcinoma *in vitro* and *in vivo* [87].

Another important metabolite produced by the serine pathway is P-Ser. Very interesting data come from the study of neural stem cell differentiation. Until a few years ago P-Ser was an orphan ligand, but recently P-Ser has been shown to bind with high affinity to the metabotropic glutamate receptor 4 and act as enhancer of neurogenesis in mammalian brain [88].
P-Ser inhibits proliferation of neural progenitor cells, promotes their fate commitment and differentiation. Further investigation on neural cell differentiation has revealed that PSPH is differentially expressed in neural progenitor cells with respect to their differentiated progeny [89]. In fact, PSPH is present only in a subset of the PHGDH-expressing cells within a small area of ongoing adult neurogenesis [90]. In this way, whereas most of cells within the neurogenic regions may synthesize P-Ser, only few of them are able to further metabolize it to L-serine, removing P-Ser from their local environment. This small number of cells avoid the P-Ser effect. Though our biologic system is not neural tissue, but a metastatic breast cancer cell line, a very important general principal is provided by the mentioned studies: through differential regulation of the serine pathway enzymes, cells are able to regulate the metabolite levels according to their needs. Likewise, variations in the serine pathway enzyme levels, like we observed in our experiments, where the first two enzymes, PHGDH and PSAT1 were upregulated, while the PSPH was down-regulated, might produce an effect similar to those of neural cells: modulation of the intracellular P-Ser level. It is currently unknown what other roles P-Ser could play in the cell, but intensive work has to be done to shed light on the involvement of let-7 miRNAs in the regulation of serine synthesis pathways.

A consideration has to be done in respect to the PSAT1 detection. Each time when we detected PSAT1 by western blot, we observed double bands. Only the lower band was strongly increased in let-7 treated samples. It might suggest the possibility of post-translational modification, like phosphorylation or methylation. At present there is no information about post-translational modifications of this enzyme in the literature, but different phosphorylation sites are predicted. However, the possibility of an unspecific upper band cannot be excluded.

Possible model of serine pathway functional role in differentiation (or other biological processes):

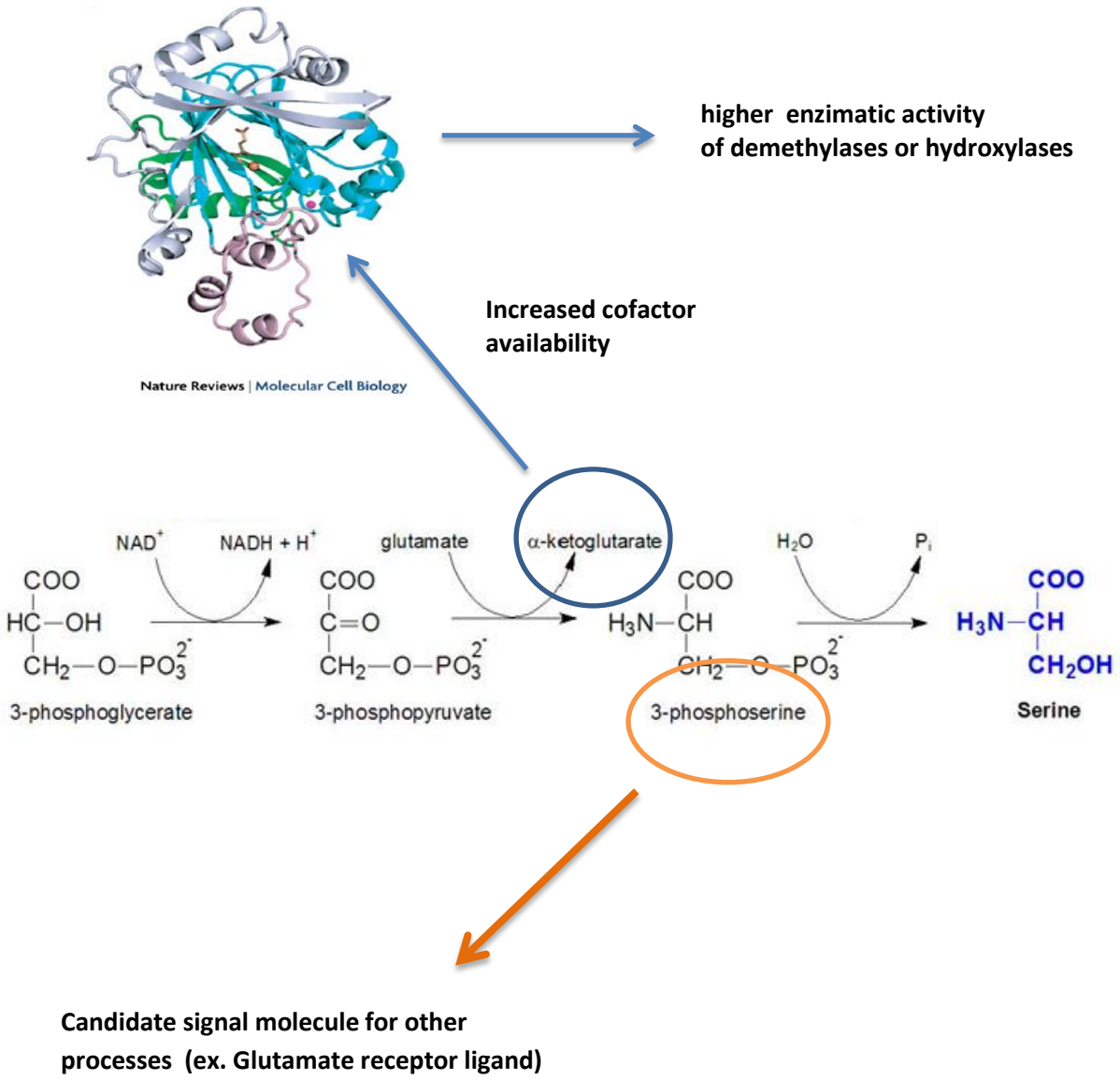

Despite the appeal of this model, for the moment there is no proof that can support this mechanism. But this hypothesis provides a starting point for further investigation of something totally new and until now unexplored.

7. CONCLUSIONS AND FUTURE PERSPECTIVES

We confirmed that *let-7* miRNA reduces cell proliferation and down-regulates HMGA2, Cyclin D1, Ras, Lin-28A and H3 in MDA-MB-231 cells. However, we did not observe recovery of epithelial markers like E-Cadherin or decrease of mesenchymal markers CD44 and vimentin.

We found that *let-7* is able to interfere with the Wnt pathway by reducing the active form of β-catenin. This adds another piece to the overall picture that defines anticancer properties of *let-7* miRNA. Many drugs currently under development target the Wnt pathway. It would be interesting to see if by combining another drug with *let-7* miRNA a synergistic effect could be obtained.

We have found a new metabolic function of *let-7* related to the serine biosynthesis pathway. We showed that in MDA-MB-231 cells components of this pathway are induced by *let-7* miRNA overexpression, coinciding with reduced proliferation. This apparent paradox suggests a possible function of this pathway beyond the synthesis of serine, for instance its involvement in differentiation, and opens new horizons for future research, and as targets for therapy.

It would be illuminating to have a global view of proteins and genes affected by *let-7* overexpression. For this purpose, global gene expression, proteomics and metabolomics studies should be done by microarray, stable isotope labeling by amino acids (SILAC) and nuclear magnetic resonance (NMR) respectively, which we already have initiated. Another goal is to extend the findings in this thesis to different breast cancer cell lines and other types of tumors to better understand how general these mechanisms are.

REFERENCES

1. Shibata, D., *Cancer. Heterogeneity and tumor history.* Science. **336**(6079): p. 304-5.
2. Al-Hajj, M., et al., *Prospective identification of tumorigenic breast cancer cells.* Proc Natl Acad Sci U S A, 2003. **100**(7): p. 3983-8.
3. Denison, T.A. and Y.H. Bae, *Tumor heterogeneity and its implication for drug delivery.* J Control Release.
4. Liu, A.Y., et al., *Stromal-epithelial interactions in early neoplasia.* Cancer Biomark. **9**(1-6): p. 141-55.
5. Mani, S.A., et al., *The epithelial-mesenchymal transition generates cells with properties of stem cells.* Cell, 2008. **133**(4): p. 704-15.
6. Sethi, S., et al., *Molecular markers of epithelial-to-mesenchymal transition are associated with tumor aggressiveness in breast carcinoma.* Transl Oncol. **4**(4): p. 222-6.
7. Oskarsson, T., et al., *Breast cancer cells produce tenascin C as a metastatic niche component to colonize the lungs.* Nat Med. **17**(7): p. 867-74.
8. Shook, D. and R. Keller, *Mechanisms, mechanics and function of epithelial-mesenchymal transitions in early development.* Mech Dev, 2003. **120**(11): p. 1351-83.
9. Montserrat, N., et al., *Epithelial to mesenchymal transition in early stage endometrioid endometrial carcinoma.* Hum Pathol. **43**(5): p. 632-43.
10. Choi, S.S. and A.M. Diehl, *Epithelial-to-mesenchymal transitions in the liver.* Hepatology, 2009. **50**(6): p. 2007-13.
11. Weijer, C.J., *Collective cell migration in development.* J Cell Sci, 2009. **122**(Pt 18): p. 3215-23.
12. Friedl, P. and D. Gilmour, *Collective cell migration in morphogenesis, regeneration and cancer.* Nat Rev Mol Cell Biol, 2009. **10**(7): p. 445-57.
13. Nabeshima, K., et al., *Cohort migration of carcinoma cells: differentiated colorectal carcinoma cells move as coherent cell clusters or sheets.* Histol Histopathol, 1999. **14**(4): p. 1183-97.
14. Giampieri, S., et al., *Localized and reversible TGFbeta signalling switches breast cancer cells from cohesive to single cell motility.* Nat Cell Biol, 2009. **11**(11): p. 1287-96.
15. Trimboli, A.J., et al., *Direct evidence for epithelial-mesenchymal transitions in breast cancer.* Cancer Res, 2008. **68**(3): p. 937-45.
16. Brabletz, T., et al., *Invasion and metastasis in colorectal cancer: epithelial-mesenchymal transition, mesenchymal-epithelial transition, stem cells and beta-catenin.* Cells Tissues Organs, 2005. **179**(1-2): p. 56-65.
17. Sato, M., D.S. Shames, and Y. Hasegawa, *Emerging evidence of Epithelial-to-Mesenchymal Transition in lung carcinogenesis.* Respirology.
18. Vergara, D., et al., *Epithelial-mesenchymal transition in ovarian cancer.* Cancer Lett. **291**(1): p. 59-66.
19. Usami, Y., et al., *Snail-associated epithelial-mesenchymal transition promotes oesophageal squamous cell carcinoma motility and progression.* J Pathol, 2008. **215**(3): p. 330-9.
20. Brabletz, T., et al., *Variable beta-catenin expression in colorectal cancers indicates tumor progression driven by the tumor environment.* Proc Natl Acad Sci U S A, 2001. **98**(18): p. 10356-61.
21. Laberge, R.M., et al., *Epithelial-mesenchymal transition induced by senescent fibroblasts.* Cancer Microenviron. **5**(1): p. 39-44.
22. Zeisberg, M. and E.G. Neilson, *Biomarkers for epithelial-mesenchymal transitions.* J Clin Invest, 2009. **119**(6): p. 1429-37.
23. Chaffer, C.L., E.W. Thompson, and E.D. Williams, *Mesenchymal to epithelial transition in development and disease.* Cells Tissues Organs, 2007. **185**(1-3): p. 7-19.
24. Kalluri, R. and R.A. Weinberg, *The basics of epithelial-mesenchymal transition.* J Clin Invest, 2009. **119**(6): p. 1420-8.
25. Turley, E.A., et al., *Mechanisms of disease: epithelial-mesenchymal transition--does cellular plasticity fuel neoplastic progression?* Nat Clin Pract Oncol, 2008. **5**(5): p. 280-90.

26. Saloman, D.S., et al., *The EGF-CFC family: novel epidermal growth factor-related proteins in development and cancer.* Endocr Relat Cancer, 2000. **7**(4): p. 199-226.
27. Valdes-Mora, F., et al., *TWIST1 overexpression is associated with nodal invasion and male sex in primary colorectal cancer.* Ann Surg Oncol, 2009. **16**(1): p. 78-87.
28. Yuen, H.F., et al., *Upregulation of Twist in oesophageal squamous cell carcinoma is associated with neoplastic transformation and distant metastasis.* J Clin Pathol, 2007. **60**(5): p. 510-4.
29. Biddle, A. and I.C. Mackenzie, *Cancer stem cells and EMT in carcinoma.* Cancer Metastasis Rev.
30. Zavadil, J. and E.P. Bottinger, *TGF-beta and epithelial-to-mesenchymal transitions.* Oncogene, 2005. **24**(37): p. 5764-74.
31. Zvaifler, N.J., *Relevance of the stroma and epithelial-mesenchymal transition (EMT) for the rheumatic diseases.* Arthritis Res Ther, 2006. **8**(3): p. 210.
32. Eisenmann, D.M., *Wnt signaling.* WormBook, 2005: p. 1-17.
33. Yamamoto, H., et al., *Wnt5a signaling is involved in the aggressiveness of prostate cancer and expression of metalloproteinase.* Oncogene. **29**(14): p. 2036-46.
34. Kurayoshi, M., et al., *Expression of Wnt-5a is correlated with aggressiveness of gastric cancer by stimulating cell migration and invasion.* Cancer Res, 2006. **66**(21): p. 10439-48.
35. Sadot, E., et al., *Regulation of S33/S37 phosphorylated beta-catenin in normal and transformed cells.* J Cell Sci, 2002. **115**(Pt 13): p. 2771-80.
36. Amit, S., et al., *Axin-mediated CKI phosphorylation of beta-catenin at Ser 45: a molecular switch for the Wnt pathway.* Genes Dev, 2002. **16**(9): p. 1066-76.
37. Vander Heiden, M.G., L.C. Cantley, and C.B. Thompson, *Understanding the Warburg effect: the metabolic requirements of cell proliferation.* Science, 2009. **324**(5930): p. 1029-33.
38. Zu, X.L. and M. Guppy, *Cancer metabolism: facts, fantasy, and fiction.* Biochem Biophys Res Commun, 2004. **313**(3): p. 459-65.
39. Berezikov, E., et al., *Phylogenetic shadowing and computational identification of human microRNA genes.* Cell, 2005. **120**(1): p. 21-4.
40. Bentwich, I., et al., *Identification of hundreds of conserved and nonconserved human microRNAs.* Nat Genet, 2005. **37**(7): p. 766-70.
41. Winter, J., et al., *Many roads to maturity: microRNA biogenesis pathways and their regulation.* Nat Cell Biol, 2009. **11**(3): p. 228-34.
42. Hutvagner, G., *Small RNA asymmetry in RNAi: function in RISC assembly and gene regulation.* FEBS Lett, 2005. **579**(26): p. 5850-7.
43. Davis-Dusenbery, B.N. and A. Hata, *MicroRNA in Cancer: The Involvement of Aberrant MicroRNA Biogenesis Regulatory Pathways.* Genes Cancer. **1**(11): p. 1100-14.
44. Viswanathan, S.R., G.Q. Daley, and R.I. Gregory, *Selective blockade of microRNA processing by Lin28.* Science, 2008. **320**(5872): p. 97-100.
45. Benhamed, M., et al., *Senescence is an endogenous trigger for microRNA-directed transcriptional gene silencing in human cells.* Nat Cell Biol. **14**(3): p. 266-75.
46. Majid, S., et al., *MicroRNA-205-directed transcriptional activation of tumor suppressor genes in prostate cancer.* Cancer, 2010. **116**(24): p. 5637-49.
47. Reinhart, B.J., et al., *The 21-nucleotide let-7 RNA regulates developmental timing in Caenorhabditis elegans.* Nature, 2000. **403**(6772): p. 901-6.
48. Pasquinelli, A.E., et al., *Conservation of the sequence and temporal expression of let-7 heterochronic regulatory RNA.* Nature, 2000. **408**(6808): p. 86-9.
49. Chang, C.J., et al., *Let-7d functions as novel regulator of epithelial-mesenchymal transition and chemoresistant property in oral cancer.* Oncol Rep. **26**(4): p. 1003-10.
50. Yu, C.C., et al., *MicroRNA let-7a represses chemoresistance and tumourigenicity in head and neck cancer via stem-like properties ablation.* Oral Oncol. **47**(3): p. 202-10.
51. Kim, S.J., et al., *MicroRNA let-7a suppresses breast cancer cell migration and invasion through downregulation of C-C chemokine receptor type 7.* Breast Cancer Res. **14**(1): p. R14.
52. Barh, D., et al., *MicroRNA let-7: an emerging next-generation cancer therapeutic.* Curr Oncol. **17**(1): p. 70-80.

53. Qian, P., et al., *Pivotal role of reduced let-7g expression in breast cancer invasion and metastasis.* Cancer Res. **71**(20): p. 6463-74.
54. Zhao, Y., et al., *let-7 MicroRNAs Induce Tamoxifen Sensitivity by Downregulation of Estrogen Receptor alpha Signaling in Breast Cancer.* Mol Med. **17**(11-12): p. 1233-41.
55. Kota, J., et al., *Therapeutic microRNA delivery suppresses tumorigenesis in a murine liver cancer model.* Cell, 2009. **137**(6): p. 1005-17.
56. Nair, V.S., L.S. Maeda, and J.P. Ioannidis, *Clinical outcome prediction by microRNAs in human cancer: a systematic review.* J Natl Cancer Inst, 2012. **104**(7): p. 528-40.
57. Cailleau, R., et al., *Breast tumor cell lines from pleural effusions.* J Natl Cancer Inst, 1974. **53**(3): p. 661-74.
58. Cailleau, R., M. Olive, and Q.V. Cruciger, *Long-term human breast carcinoma cell lines of metastatic origin: preliminary characterization.* In Vitro, 1978. **14**(11): p. 911-5.
59. Davis, H.E., et al., *Charged polymers modulate retrovirus transduction via membrane charge neutralization and virus aggregation.* Biophys J, 2004. **86**(2): p. 1234-42.
60. Klopp, A.H., et al., *Mesenchymal stem cells promote mammosphere formation and decrease E-cadherin in normal and malignant breast cells.* PLoS One. **5**(8): p. e12180.
61. Yu, F., et al., *let-7 regulates self renewal and tumorigenicity of breast cancer cells.* Cell, 2007. **131**(6): p. 1109-23.
62. Ganapathy-Kanniappan, S., et al., *Human hepatocellular carcinoma in a mouse model: assessment of tumor response to percutaneous ablation by using glyceraldehyde-3-phosphate dehydrogenase antagonists.* Radiology. **262**(3): p. 834-45.
63. Possemato, R., et al., *Functional genomics reveal that the serine synthesis pathway is essential in breast cancer.* Nature. **476**(7360): p. 346-50.
64. Martens, J.W., et al., *Association of DNA methylation of phosphoserine aminotransferase with response to endocrine therapy in patients with recurrent breast cancer.* Cancer Res, 2005. **65**(10): p. 4101-17.
65. Vie, N., et al., *Overexpression of phosphoserine aminotransferase PSAT1 stimulates cell growth and increases chemoresistance of colon cancer cells.* Mol Cancer, 2008. **7**: p. 14.
66. Pollari, S., et al., *Enhanced serine production by bone metastatic breast cancer cells stimulates osteoclastogenesis.* Breast Cancer Res Treat, 2011. **125**(2): p. 421-30.
67. Johnson, S.M., et al., *RAS is regulated by the let-7 microRNA family.* Cell, 2005. **120**(5): p. 635-47.
68. Lee, Y.S. and A. Dutta, *The tumor suppressor microRNA let-7 represses the HMGA2 oncogene.* Genes Dev, 2007. **21**(9): p. 1025-30.
69. Ricarte-Filho, J.C., et al., *Effects of let-7 microRNA on Cell Growth and Differentiation of Papillary Thyroid Cancer.* Transl Oncol, 2009. **2**(4): p. 236-41.
70. Legesse-Miller, A., et al., *let-7 Overexpression leads to an increased fraction of cells in G2/M, direct down-regulation of Cdc34, and stabilization of Wee1 kinase in primary fibroblasts.* J Biol Chem, 2009. **284**(11): p. 6605-9.
71. Ren, H. and H. Zhang, *Wnt signaling controls temporal identities of seam cells in Caenorhabditis elegans.* Dev Biol. **345**(2): p. 144-55.
72. Doble, B.W. and J.R. Woodgett, *GSK-3: tricks of the trade for a multi-tasking kinase.* J Cell Sci, 2003. **116**(Pt 7): p. 1175-86.
73. Zhu, H., et al., *The Lin28/let-7 axis regulates glucose metabolism.* Cell, 2011. **147**(1): p. 81-94.
74. Byers, S., et al., *Retinoids increase cell-cell adhesion strength, beta-catenin protein stability, and localization to the cell membrane in a breast cancer cell line: a role for serine kinase activity.* Endocrinology, 1996. **137**(8): p. 3265-73.
75. Barbatelli, G., et al., *The emergence of cold-induced brown adipocytes in mouse white fat depots is determined predominantly by white to brown adipocyte transdifferentiation.* Am J Physiol Endocrinol Metab, 2010. **298**(6): p. E1244-53.
76. Seo, E.Y., et al., *Identification of calcium-inducible genes in primary keratinocytes using suppression-subtractive hybridization.* Exp Dermatol, 2004. **13**(3): p. 163-9.

77. Bachelor, M.A., Y. Lu, and D.M. Owens, *L-3-Phosphoserine phosphatase (PSPH) regulates cutaneous squamous cell carcinoma proliferation independent of L-serine biosynthesis.* J Dermatol Sci. **63**(3): p. 164-72.
78. Lund, K., D.K. Merrill, and R.W. Guynn, *The reactions of the phosphorylated pathway of L-serine biosynthesis: thermodynamic relationships in rabbit liver in vivo.* Arch Biochem Biophys, 1985. **237**(1): p. 186-96.
79. Fallon, H.J., *Regulatory phenomena in mammalian serine metabolism.* Adv Enzyme Regul, 1967. **5**: p. 107-20.
80. Korpal, M., et al., *The miR-200 family inhibits epithelial-mesenchymal transition and cancer cell migration by direct targeting of E-cadherin transcriptional repressors ZEB1 and ZEB2.* J Biol Chem, 2008. **283**(22): p. 14910-4.
81. Gregory, P.A., et al., *The miR-200 family and miR-205 regulate epithelial to mesenchymal transition by targeting ZEB1 and SIP1.* Nat Cell Biol, 2008. **10**(5): p. 593-601.
82. Donohoe, D.R. and S.J. Bultman, *Metaboloepigenetics: Interrelationships between energy metabolism and epigenetic control of gene expression.* J Cell Physiol, 2012. **227**(9): p. 3169-77.
83. Parsons, D.W., et al., *An integrated genomic analysis of human glioblastoma multiforme.* Science, 2008. **321**(5897): p. 1807-12.
84. Yan, H., et al., *IDH1 and IDH2 mutations in gliomas.* N Engl J Med, 2009. **360**(8): p. 765-73.
85. Mardis, E.R., et al., *Recurring mutations found by sequencing an acute myeloid leukemia genome.* N Engl J Med, 2009. **361**(11): p. 1058-66.
86. Rzeski, W., et al., *Alpha-ketoglutarate (AKG) inhibits proliferation of colon adenocarcinoma cells in normoxic conditions.* Scand J Gastroenterol. **47**(5): p. 565-71.
87. Matsumoto, K., et al., *Antitumor effects of 2-oxoglutarate through inhibition of angiogenesis in a murine tumor model.* Cancer Sci, 2009. **100**(9): p. 1639-47.
88. Saxe, J.P., et al., *A phenotypic small-molecule screen identifies an orphan ligand-receptor pair that regulates neural stem cell differentiation.* Chem Biol, 2007. **14**(9): p. 1019-30.
89. Geschwind, D.H., et al., *A genetic analysis of neural progenitor differentiation.* Neuron, 2001. **29**(2): p. 325-39.
90. Nakano, I., et al., *Phosphoserine phosphatase is expressed in the neural stem cell niche and regulates neural stem and progenitor cell proliferation.* Stem Cells, 2007. **25**(8): p. 1975-84.

ATTACHMENT N1

List of primary Ab used for western blotting

Ab	Source	Dilutions	Catalog number
Actin	Santa Cruz	1:500	sc-1616
Active β-catenin	Cell signaling	1:500	05-665
CD24 PE conjugated	BD Pharmingen	1:20	555428
CD44 FITC conjugated	BD Pharmingen	1:20	347943
Cyclin D1	Cell signaling	1:2000	2926
Histone 3	Millipore	1:10000	05-928
HMGA2	SDI	1:10000	25810002
Lin28A	Proteintech Group	1:1000	3978
Ph- β-catenin	Cell signaling	1:1000	9561
PHGDH	Santa Cruz	1:1000	Sc-100317
PSAT1	GeneTex	1:1000	GTX115909
PSPH	Santa Cruz	1:100	sc-74827
Ras	Cell signaling	1:1000	3965
Total β-catenin	Abcam	1:1000	ab 16051
α-tubulin	Calbiochem	1:2000	CP06